Plant Cell Advance Publication. Published on July 18, 2016, doi:10.1105/tpc.16.00193

Metabolite diversity in alkaloid biosynthesis: A multi-lane (diastereomer) highway for camptothecin synthesis in *Camptotheca acuminata*

Radin Sadre[a], Maria Magallanes-Lundback[a], Sujana Pradhan[b,c], Vonny Salim[a,c], Alex Mesberg[a], A. Daniel Jones[a,b] and Dean DellaPenna[a]

[a] Department of Biochemistry and Molecular Biology, Michigan State University, East Lansing, Michigan 48824-1319

[b] Department of Chemistry, Michigan State University, East Lansing, Michigan 48824-1319

[c] contributed equally

Corresponding author: Dean DellaPenna (dellapen@msu.edu)

Short title: Camptothecin biosynthesis in *Camptotheca*

The author responsible for distribution of materials integral to the findings presented in this article in accordance with the policy described in the Instructions for Authors (www.plantcell.org) is: Dean DellaPenna (dellapen@msu.edu)

Synopsis**:** Unlike previously characterized MIA producing plants, *Camptotheca acuminata* uses an alternative seco-iridoid pathway to form diastereomer intermediates for the biosynthesis of the MIA camptothecin.

ABSTRACT

Camptothecin is a monoterpene indole alkaloid (MIA) used to produce semi-synthetic anti-tumor drugs. We investigated camptothecin synthesis in *Camptotheca acuminata* by combining transcriptome and expression data with reverse genetics, biochemistry, and metabolite profiling. RNAi silencing of enzymes required for the indole and seco-iridoid (monoterpene) components identified transcriptional cross-talk coordinating their synthesis in roots. Metabolite profiling and labeling studies of wild type and RNAi lines identified plausible intermediates for missing pathway steps and demonstrated nearly all camptothecin pathway intermediates are present as multiple isomers. Unlike previously characterized MIA-producing plants, *C. acuminata* does not synthesize 3-alpha(*S*)-strictosidine as its central MIA intermediate and instead uses an alternative seco-iridoid pathway that produces multiple isomers of strictosidinic acid. NMR analysis demonstrated that the two major strictosidinic acid isomers are (*R*) and (*S*) diastereomers at their glucosylated C21 positions. The presence of multiple diastereomers throughout the pathway is consistent with their use in synthesis before finally being resolved to a single camptothecin isomer after deglucosylation, much as a multi-lane highway allows parallel tracks to converge at a common destination. A model "diastereomer" pathway for camptothecin biosynthesis in *C. acuminata* is proposed that fundamentally differs from previously studied MIA pathways.

INTRODUCTION

Monoterpene indole alkaloids (MIA) account for thousands of specialized metabolites produced by plant species from the orders Cornales and Gentianales. Much of this chemical diversity originates from the common precursor 3-alpha(*S*)-strictosidine, which is formed by stereospecific condensation of the indole metabolite tryptamine and the monoterpene secologanin (De Luca et al., 2014). MIA metabolic diversity likely evolved as components of plant adaptation to changing environments and as defensive agents against various biotic stresses. Many MIAs, including camptothecin, target specific cellular processes in mammals and have important pharmacological activities and medicinal uses. Camptothecin was first identified during the 1960s as a novel antitumor alkaloid of *Camptotheca acuminata* (Cornales), a tree native to Southern China (Wall et al., 1966). Its mode of action is the specific inactivation of topoisomerase I resulting in cell death by apoptosis (Wright et al., 2015). Semi-synthetic analogs derived from camptothecin exhibit improved pharmacological properties and clinical efficacy relative to camptothecin, and are widely used to treat lung, colorectal, cervical and ovarian cancers (Liu et al., 2015). As for many alkaloids, chemical synthesis of camptothecin is impractical and the production of semi-synthetic derivatives relies entirely on camptothecin isolated from the bark and seeds of *C. acuminata* and *Nothapodytes nimmoniana* (Lorence and Nessler, 2004). The increasing worldwide demand for camptothecin requires exploration of more economical and sustainable alternatives for its production.

Despite the medicinal importance of camptothecin, its biosynthesis by plants remains undeciphered. Since its original discovery in *C. acuminata*, camptothecin was found to accumulate in several Asian and African tropical and subtropical plant species from unrelated orders and families, including species of *Ophiorrhiza* (Wink, 2003; Gopalakrishnan and Shankar, 2014). Early radiolabeling experiments in *C. acuminata* demonstrated that tryptophan and its decarboxylation product tryptamine were metabolic precursors, as was a mixture of the monoterpene alcohols geraniol and its *cis*-isomer nerol, leading to classification of camptothecin as a MIA (Sheriha and Rapoport, 1976) despite it having a quinoline, and not indole, ring system. Subsequent stable isotope labeling and NMR experiments demonstrated that strictosamide served as a precursor for camptothecin in *C. acuminata* (Hutchinson et al., 1979).

The co-occurrence of camptothecin in *Ophiorrhiza pumila* with the structurally related alkaloids pumiloside and deoxypumiloside suggested they are intermediates in the camptothecin biosynthetic pathway (Aimi et al., 1989). Notably, pumiloside was also detected in *C. acuminata* (Carte et al., 1990, Montoro et al. 2010). Recent studies of camptothecin biosynthesis in *O. pumila* hairy roots demonstrated that strictosidine, derived from the condensation of tryptamine and the seco-iridoid secologanin, is required for camptothecin synthesis in this species (Asano et al., 2013; Yamazaki et al., 2013).

The seco-iridoid pathway leading to strictosidine was only recently elucidated in the MIA producing plant *Catharanthus roseus*. Geraniol 8-oxidase (CYP76B6) catalyzes hydroxylation of the MEP pathway-derived isoprenoid geraniol to 8-hydroxygeraniol, which undergoes further oxidation to the di-aldehyde 8-oxogeranial (**1**) by 8-hydroxygeraniol oxidoreductase (Hofer et al., 2013). The enzyme iridoid synthase catalyzes the subsequent conversion of 8-oxogeranial (**1**) to iridodial (Geu-Flores et al., 2012), which is oxidized further to 7-deoxyloganetic acid by 7-deoxyloganetic acid synthase (CYP76A26) (Salim et al., 2014). 7-Deoxyloganetic acid is glycosylated to 7-deoxyloganic acid (Asada et al., 2013), which undergoes subsequent hydroxylation by CYP72A224 to yield loganic acid, whose carboxyl group is then *O*-methylated to form loganin (Murata et al., 2008; Salim et al., 2013). Secologanin synthase (CYP72A1) then catalyzes the oxidative ring-opening of loganin to secologanin, which contains an aldehyde group suitable for condensation with the amino group of tryptamine (Irmler et al., 2000). Strictosidine synthase, a Pictet-Spenglerase, catalyzes the stereospecific condensation of tryptamine and secologanin to 3-alpha(*S*)-strictosidine (Bracher and Kutchan, 1992). It was proposed that strictosidine is subsequently channeled into the biosynthesis of the downstream MIAs strictosamide, pumiloside and deoxypumiloside to yield camptothecin in *O. pumila* (Asano et al., 2013). However, post-strictosidine reaction steps, enzymes and their sequence(s) remain unknown in camptothecin-producing plants.

The Medicinal Plant Consortium recently made the assembled transcriptome, gene expression and metabolite profiles for *C. acuminata* publicly available (http://medicinalplantgenomics.msu.edu/, http://metnetdb.org/mpmr_public/). Here, we combined analyses of transcriptome and expression datasets with reverse genetics, biochemistry and metabolite profiling to investigate camptothecin biosynthesis in soil-grown *C. acuminata*

plants. Two essential genes for camptothecin biosynthesis, those encoding tryptophan decarboxylase and iridoid synthase, were identified and down-regulated by RNAi, and the consequences for metabolite and gene expression profiles determined. Our key findings are that in contrast to other well-studied MIA producing plants, including *O. pumila* (Yamazaki et al., 2003b; Asano et al., 2013), *C. acuminata* does not synthesize strictosidine and instead uses an alternative seco-iridoid pathway to produce strictosidinic acid composed of a mixture of glucoside diastereomers varying in stereochemistry at C21. These strictosidinic acid diastereomers are channeled into the camptothecin pathway and multiple diastereomers of other intermediates are present throughout the pathway, comparable to a multi-lane highway in which parallel lanes lead to a single destination, in this case a single isomer of camptothecin. Finally, we identify novel alkaloids that are plausible intermediates for missing steps in the pathway using stable isotope labeling and tandem mass spectrometry.

RESULTS

Identification and characterization of camptothecin pathway intermediates in *C. acuminata*

To assess the abundance of putative intermediates of the camptothecin pathway in *C. acuminata*, five different tissues (root, green stems, shoot apex and young and mature leaves) were collected from wild type plants grown under greenhouse conditions, and 70% aqueous acetonitrile extracts were subjected to non-targeted UHPLC/MS analysis using a 52-min reverse phase chromatographic separation. Nineteen metabolites were annotated based on accurate mass measurements of positive ions and fragments observed in UHPLC/MS and UHPLC/MS/MS mass spectra (Figure 1, Table 1, Supplemental Table S1). Wild-type *C. acuminata* accumulated tryptamine (**4**), the iridoids loganic acid (**2**) and secologanic acid (**3**) as well as the MIA strictosidinic acid (**5**), but lacked detectable levels of their methyl-esterified derivatives loganin, secologanin and strictosidine (numbers in bold numbers correspond to the chemical structures shown in Table 1 and Figure 1). This suggests that in contrast to the best-studied MIA producing plants *Rauvolfia serpentina* and *C. roseus* that use methyl-esterified intermediates (De Luca et al., 2014), *C. acuminata* uses an alternative seco-iridoid pathway with carboxylic acid intermediates up to strictosidinic acid. Several post-strictosidinic acid metabolites that we

132 propose as intermediates in the camptothecin pathway were also detected (Table 1). In addition
133 to the previously reported metabolites strictosamide (**6**) and pumiloside (**10**) (Hutchinson et al.,
134 1979; Carte et al., 1990; Montoro et al., 2010), we identified metabolites with exact molecular
135 masses and fragment ions consistent with strictosamide epoxide (**7**), strictosamide diol (**8**),
136 strictosamide ketolactam (**9**), and deoxypumiloside (**11**) (Table 1). Surprisingly, most of these
137 MIAs were present in multiple isomeric forms with identical exact molecular and fragment ion
138 masses that we resolved and numbered according to their relative elution order. Note that all
139 isomers of a compound have the same bolded number and that additional descriptors are used to
140 differentiate isomers (e.g. isomer 1 and isomer 2). Strictosidinic acid (**5**) and strictosamide
141 epoxide (**7**) each exhibited three isomers, while two isomers each were detected for strictosamide
142 (**6**), strictosamide ketolactam (**9**), pumiloside (**10**) and deoxypumiloside (**11).**
143 We next quantified the relative levels of these metabolites and their isomers that could be
144 detected in extracts of five different tissues for three wild type plants (Figure 2). As expected,
145 shoot apex and young leaf shared similar metabolite profiles and accumulated most metabolites
146 at distinctly higher levels compared to root and/or mature leaf. Tryptamine (**4**) was only detected
147 in stem, shoot apex and young leaf. Loganic acid (**2**) content was highest in stem, lower in other
148 photosynthetic tissues and absent from root. Secologanic acid (**3**) was detected in all five tissues
149 with levels in photosynthetic tissues two- to three-fold higher than in roots. The major
150 accumulation sites for strictosidinic acid (**5**) were shoot apex and young leaf with progressively
151 lower levels in stem, root and mature leaf. Surprisingly, the levels of strictosamide (**6**) were
152 nearly identical in all tissues. Strictosamide epoxide (**7**), strictosamide diol (**8**), and strictosamide
153 ketolactam (**9**) could not be reliably quantified due to their low abundances in all *C. acuminata*
154 tissues. The tissue distribution profile of pumiloside (**10**) was similar to that of strictosidinic acid
155 (**5**), with the highest levels being in shoot apex and young leaf and lowest levels in mature leaf.
156 Deoxypumiloside (**11**) was only detected in stem, root and at extremely low levels in shoot apex.
157 All tissues contained camptothecin (**12**) with young leaf and shoot apex accumulating the highest
158 levels. It is noteworthy that the relative amounts of isomers of strictosidinic acid (**5**) and post-
159 strictosidinic acid intermediates varied among tissues (Figure 2). In most tissues, one of the two
160 major isomers was more abundant; for example, strictosamide (**6**) isomer 1 predominates in roots

161 and stems, while isomer 2 predominates in shoot apices and leaves. In general, roots and stems
162 have similar isomer profiles as do young and mature leaves.
163 The presence of multiple isomeric MIA metabolites in UHPLC/MS metabolite profiles of
164 *C. acuminata* tissues with indistinguishable MS/MS spectra (Table 1, Supplemental Table S1)
165 suggested they differ in stereochemical configurations, but their chromatographic resolution
166 indicates they are diastereomers. To assess the nature of these isomeric compounds, the two most
167 abundant isomers of strictosidinic acid (**5**), which were present in sufficient quantity to be
168 purified, were subjected to an assortment of 1- and 2-dimensional NMR spectroscopic analyses.
169 The most substantial differences were observed in the ^{1}H chemical shifts at position 21 (Table 2,
170 Supplemental Data Set S1), which is the position of glycosylation. Subsequent coupled
171 Heteronuclear Single Quantum Coherence (cHSQC) NMR spectra were generated to assess
172 whether relative stereochemical configuration of hydrogens at chiral positions could be assessed
173 by measuring the ^{1}H-^{13}C coupling constants, which are sensitive to orientation relative to other
174 bonds, and have been used to establish relative bond orientations in a variety of metabolites
175 (Marquez et al. 2001). These coupling constants ($^{1}J_{C\text{-}H}$) were 170 Hz for isomer 2 and 178 Hz for
176 isomer 3, the largest isomer-related difference among all $^{1}J_{C\text{-}H}$ values and consistent with two
177 epimers differing in the stereochemistry of C-glycosylation at position 21 (Figure 3, Table 2).
178 Based on similarities to NMR spectra reported for 21(*S*)-strictosidine, we assign strictosidinic
179 acid isomer 3 to have the 21(*R)* configuration and strictosidinic acid isomer 2 to have 21(*S)*
180 configuration (Figure 3), the latter being in common with the published structure and coupling
181 constants of 21(*S)*-strictosidine (Patthy-Lukáts et al. 1997). NMR data for stereocenters at
182 positions 3, 15, 20, and the carbohydrate resonances for isomers 2 and 3 did not differ
183 substantially, consistent with the difference being the configuration at position 21. These two
184 diastereomer configurations are most likely formed earlier in iridoid biosynthesis by the
185 spontaneous ring opening and closing of 7-deoxyloganetic acid that forms C2-hydroxy epimers,
186 which are then glycosylated (Figure 4). The presence of multiple isomers for most of the later
187 biosynthetic intermediates suggests that *C. acuminata* 7-deoxyloganetic acid glucosyltransferase
188 is either a promiscuous enzyme that can accommodate both *R*- and *S*-isomers of 7-
189 deoxyloganetic acid or that multiple stereospecific *C. acuminata* 7-deoxyloganetic acid
190 glycosyltransferases exist. Under our 52-min chromatographic conditions, the first iridoids we

can detect, loganic acid (**2**) and secologanic acid (**3**), appeared as single chromatographic peaks; however, two isomers were resolved for each using a different chromatography column and gradient (Supplemental Figure S1 and Supplemental Figure S2). Thus, the isomers observed throughout the pathway are likely glucosidic isomers that have their origin early in iridoid synthesis.

On the basis of these observations, a model pathway for camptothecin synthesis in *C. acuminata* is proposed (Figure 1), where tryptamine (**4**) and the aldehyde-containing iridoid secologanic acid (**3**) (rather than secologanin) are coupled via a Pictet-Spengler reaction, leading to strictosidinic acid (**5**). Intramolecular dehydrative cyclization of strictosidinic acid yields strictosamide (**6**). Conversion of the indole ring system to the quinoline ring is postulated to occur via multi-step oxidation to strictosamide ketolactam (**9**) followed by condensation and elimination of water to yield the quinolinone ring of pumiloside (**10**). The subsequent reduction to deoxypumiloside (**11**), deglycosylation, and other metabolic conversions lead to the end product camptothecin (**12**). This model pathway takes into account the formation and retention of multiple glycosidic isomers (diastereomers) for pathway intermediates from 7-deoxyloganetic acid to deoxypumiloside (**11**).

Identification of candidate genes involved in camptothecin biosynthesis

Genes responsible for the production of camptothecin in *C. acuminata* are largely unknown. A previous study demonstrated that *C. acuminata* possesses two differentially expressed tryptophan decarboxylase genes, *TDC1* and *TDC2*, for the synthesis of tryptamine (Lopez-Meyer and Nessler, 1997). Transcriptome data from the Medicinal Plant Genomics Resource (MPGR) database (Gongora-Castillo et al., 2012) indicated that *TDC1* expression is moderate to high in leaves, roots and young bark of *C. acuminata,* while *TDC2* transcript is barely detectable in most plant tissues, with the exception of immature and mature fruit. In mature leaves, roots and young bark, *TDC1* transcript levels are 100-fold, 200-fold and 600-fold, respectively, higher than *TDC2* transcript levels. Since *TDC1* is expressed in tissues that accumulate camptothecin, we considered it the most promising candidate for synthesizing the indole precursor of camptothecin. The predicted TDC1 protein shares 68% and 74% sequence

identities with the tryptophan decarboxylases of *C. roseus* (De Luca et al., 1989) and *O. pumila* (Yamazaki et al., 2003a), respectively.

To select additional candidate camptothecin biosynthesis genes, the MPGR transcriptome data were used for co-expression analyses. We postulated that seco-iridoid pathway genes would be co-expressed with *TDC1* to coordinate synthesis of the seco-iridoid and indole precursors needed for camptothecin production. The original MPGR data set included developmental and tissue-specific expression profiles for 53,154 unique *C. acuminata* transcripts in 18 tissues from different developmental stages such as 10-day-old seedlings to fruiting trees (Gongora-Castillo et al., 2012b). Prior to co-expression analysis, genes exhibiting low transcript abundances ($\log_2$ FPKM lower than 2) in root or immature bark were removed from the data set, leaving 26,874 unique transcripts for further analyses. Additionally, as iridoid synthesis is known to involve cyclization, oxidation and glycosylation reactions (Miettinen et al., 2014), 1,146 transcripts encoding putative proteases, histone and histone-modifying proteins, ribosomal proteins, tRNA synthetases and proteins related to ubiquitinylation were considered unlikely to have direct involvement in specialized metabolism and were also removed, leaving a dataset of 25,725 transcripts for hierarchical cluster analyses.

Hierarchical cluster analysis identified a subcluster of 23 transcripts that encode 7 proteins with highest identity to known steps in the seco-iridoid pathway. These include geraniol-8-oxidase (G8O), CYCLASE 1 (CYC1) and CYCLASE 2 (CYC2), which are members of the progesterone 5-beta-reductase family, 7-deoxyloganetic acid synthase (7-DLS) and glucosyltransferase (7-DLGT), a putative ortholog of the *C. roseus* iridoid transcription factor bHLH IRIDOID SYNTHESIS 1 (BIS1) (Van Moerkercke et al. 2015) along with a putative ortholog to protein S, an α/β-hydrolase superfamily protein associated with seco-iridoid/MIA synthesizing cells in *C. roseus* (Leménager et al., 2005) (Figure 5). Like *TDC1*, most of the seco-iridoid pathway candidate genes in this cluster showed moderate to high expression in root and immature bark, but they also had lower expression than *TDC1* in other tissues (e.g., mature leaf), which resulted in their clustering apart from *TDC1* (Figure 4). The tryptophan and MEP pathways provide substrates from intermediary metabolism for tryptamine and iridoid synthesis, respectively. To assess whether members of these pathways have expression patterns similar to that of the iridoid cluster, *C. acuminata* transcripts encoding steps of the tryptophan and MEP

pathways were identified by homology searches (Supplemental Data Set S2) and their expression profiles subjected to hierarchical cluster analysis together with transcripts of the iridoid subcluster (Supplemental Figure S3, Supplemental Data Set S3). This analysis showed that the expression pattern of most tryptophan and MEP pathway genes is quite different from that of the iridoid subcluster, with a few notable exceptions: one gene encoding a tryptophan synthase subunit and one gene encoding an anthranilate synthase subunit.

CYC1 shows iridoid synthase activity in vitro

In *C. roseus*, iridoid synthase is a member of the progesterone 5-beta-reductase family that catalyzes the NAD(P)H-dependent conversion of 8-oxogeranial (**1**) to iridodial/nepetalactol in MIA biosynthesis (Geu-Flores et al., 2012; Munkert et al., 2014). This suggested that one or both of the *C. acuminata* progesterone 5-beta-reductase family members in our gene cluster (Figure 5, CYC1 and CYC2) might encode orthologous iridoid synthase activities in camptothecin biosynthesis. The *C. acuminata* transcriptome encodes at least seven progesterone 5-beta-reductase family members of which *CYC1* and *CYC2*, with 65% and 59% amino acid sequence identity, respectively, have the highest identities to *C. roseus* iridoid synthase. In comparative analysis of the phylogenetic relationships between predicted members of the progesterone-5 beta reductase family in *C. roseus*, *C. acuminata* and *R. serpentina,* CYC1 and CYC2 formed separate, well-resolved clades (Supplemental Figure S4, Supplemental Data Set S4).

To examine the catalytic activities of CYC1 and CYC2 in comparison to the previously characterized *C. roseus* iridoid synthase (Geu-Flores et al., 2012), the respective coding sequences were expressed in *Escherichia coli* and recombinant His-tagged proteins purified by affinity chromatography. The purified enzymes were subsequently tested in colorimetric dehydrogenase assays for protein functionality that are based on the NAD(P)H-dependent reduction of nitroblue tetrazolium chloride to the dark blue formazan product. These experiments indicated that all three enzymes were functional and required NAD(P)H as cofactor for activity (Supplemental Figure S5). The purified proteins were then assayed for iridoid synthase activity

with 8-oxogeranial (**1**) as substrate using a chemically synthesized substrate (Geu-Flores et al., 2012) composed of a mixture of the cis-trans isomers 8-oxogeranial (**1**)/8-oxoneral in an approximate 2:1 ratio. Incubation of CYC1 with substrate and NADPH resulted in nearly complete conversion of the substrate to seven *cis-trans* isomers of iridodial/nepetalactol that were indistinguishable in gas chromatographic retention times and mass spectra to those obtained with the *C. roseus* iridoid synthase control (Figure 6). These data clearly demonstrated that like *C. roseus* iridoid synthase, *C. acuminata* CYC1 catalyzes the reductive cyclization of 8-oxogeranial (**1**). Assays with CYC2 did not result in any detectable products, indicating that CYC2 may not use 8-oxogeranial (**1**) as substrate *in planta* (Figure 6).

Silencing of *CYC1* and *TDC1* expression in *C. acuminata* plants

CYC1 and *TDC1* were selected as targets for reverse genetics analyses by gene silencing. We developed a stable transformation method to integrate RNAi-mediating expression cassettes into the *C. acuminata* genome using the pHellsgate12 system (Helliwell and Waterhouse, 2005). *C. acuminata* cotyledon explants were transformed by *Agrobacterium tumefaciens* harboring RNAi constructs for *TDC1* or *CYC1* and transgenic plants were regenerated *in vitro*. Rooted antibiotic-resistant plantlets were transferred from *in vitro* culture to soil cultivation under greenhouse conditions. With the exception of decreased resistance to red spider mite infestation, RNAi plants did not show any obvious phenotypic differences compared to wild type plants (Supplemental Figure S6).

After a growth and acclimation period of three to four months under greenhouse cultivation, RNAi-mediated suppression of the target genes was evaluated in independent transformation events by quantitative real-time PCR. Since *TDC1* and *CYC1* expression in wild type plants is highest in immature bark, stem tissue was used to determine mRNA abundances for target genes in RNAi plants relative to untransformed wild-type control plants. In the six *TDC1*-RNAi plants analyzed, *TDC1* stem transcript levels were decreased to as low as 3% of wild type levels (Figure 7 A). Consistent with this observation, camptothecin levels in mature leaves of *TDC1*-RNAi plants were reduced by as much as 1000-fold compared to wild type plants (Figure 7 A). Similar analyses were performed on nineteen *CYC1*-RNAi plants where a much wider range of

308 silencing and impact on leaf camptothecin levels was observed (Figure 7 B). Approximately half
309 of the *CYC1*-RNAi lines had stem *CYC1* transcript levels below 15% of wild type. This group of
310 *CYC1*-RNAi lines also had 15- to 400-fold lower camptothecin levels in mature leaves than did
311 wild type plants. Taken together, these data indicate that stable RNAi transformation was
312 successful in *C. acuminata* and that the expression of both *TDC1* and *CYC1* are necessary for
313 camptothecin biosynthesis.

314 Target gene impact was further examined in five independent transformed lines of *TDC1*-
315 RNAi and *CYC1*-RNAi that had severely reduced mature leaf camptothecin levels and three wild
316 type lines independently regenerated through tissue culture. Plants used for these studies had
317 been under greenhouse cultivation for about eight months. RNA was extracted from roots, green
318 stems and young developing leaves, and the average *TDC1* and *CYC1* mRNA levels were
319 compared (Figure 8). In wild type plants, *TDC1* transcript levels were approximately 2-fold
320 higher in stems than roots and young leaves and barely detectable in these tissues in *TDC1*-RNAi
321 lines (Figure 8 A). *CYC1* expression in wild type plants was highest in stems and approximately
322 40-fold that of roots and young leaves (Figure 8 B). The average *CYC1* mRNA level in green
323 stems of *CYC1*-RNAi lines was strongly reduced to 4% of wild type while in roots and young
324 leaves it was only reduced to 49% and 27% of wild type levels, respectively, suggesting that
325 target-gene silencing was less effective in these two tissues (Figure 8 B).
326

327 ***TDC1*-RNAi plants are deficient in indole alkaloids and accumulate loganic acid in roots**

328 To further evaluate the impact of *TDC1* gene silencing on camptothecin biosynthesis,
329 extracts from roots, stems, shoot apices and young and mature leaves were subjected to
330 UHPLC/MS analyses. In contrast to the wild type controls, *TDC1*-RNAi lines did not
331 accumulate detectable levels of tryptamine (**4**), strictosidinic acid (**5**) or any of the post-
332 strictosidinic acid metabolites in Figure 1, including the newly proposed pathway intermediates
333 strictosamide epoxide (**7**), strictosamide diol (**8**) and strictosamide ketolactam (**9**). By contrast,
334 the levels of the iridoids loganic acid (**2**) and secologanic acid (**3**) in stems, shoot apices and
335 leaves of *TDC1*-RNAi plants were not significantly different from wild type levels (Figure 9).

336 However, all *TDC1*-RNAi lines accumulated loganic acid (**2**) in roots, a metabolite below
337 detection in wild type roots (Figure 9).

338 To assess whether the absence of strictosidinic acid (**5**) and post-strictosidinic acid
339 metabolites in the *TDC1*-RNAi lines was directly attributable to tryptamine (**4**) deficiency,
340 feeding experiments with deuterated tryptamine were carried out. Apical cuttings from *TDC1*-
341 RNAi and wild type plants were incubated in aqueous solutions with or without tryptamine-
342 α,α,β,β-d_4. After six weeks, stems and mature leaves were collected and extracts prepared and
343 analyzed via UHPLC/MS. As expected, incubation of wild-type apical cuttings with deuterated
344 tryptamine resulted in little incorporation of label into camptothecin pathway intermediates due
345 to the substantial intrinsic pool of unlabeled tryptamine in stem and shoot apex (approximately
346 100 nmol per gram fresh weight, Figure 2). However, when *TDC1*-RNAi cuttings were
347 incubated with deuterated tryptamine, deuterium-labeled camptothecin pathway intermediates
348 were detected in stems, and to a lesser extent in leaves. Four deuterium atoms from tryptamine-
349 d_4 were incorporated into strictosidinic acid (**5**) isomers 2 and 3 and strictosamide (**6**) isomers 1
350 and 2, while two deuterium atoms were incorporated into pumiloside (**10**) isomer 1,
351 deoxypumiloside (**11**) isomers 1 and 2 and camptothecin (**12**), providing further evidence for the
352 role of these metabolites as intermediates in camptothecin synthesis (Table 1). Because the
353 absolute levels of all pathway compounds in deuterated tryptamine *TDC1*-RNAi cuttings were
354 still much lower than in wild-type cuttings, incorporation of label into less abundant isomers
355 could not be reliably determined. The likely positions of deuterium labels within the different
356 pathway intermediates are indicated in Figure 1.
357

358 **Impaired indole alkaloid biosynthesis in *CYC1*-RNAi plants is accompanied by increased**
359 **tryptamine levels**

360 We similarly assessed the impact of *CYC1*-RNAi by analyzing pathway metabolite levels
361 in roots, stems, shoot apices and young and mature leaves of five independent *CYC1*-RNAi lines
362 in comparison to wild type. In addition to a sharp reduction in camptothecin levels in all tissues
363 to as low as 2% of wild type levels, all tissues of *CYC1*-RNAi lines accumulated substantially
364 higher levels of tryptamine (**4**) compared to wild type (Figure 9). In contrast to wild type and

365 *TDC1*-RNAi plants, which lacked detectable levels of tryptamine in roots and mature leaves,
366 *CYC1*-RNAi roots and mature leaves contained about 250 nmol tryptamine per gram fresh
367 weight (Figure 9). In stems, shoot apices, and young leaves of the *CYC1*-RNAi lines, tryptamine
368 levels approached or exceeded 1000 nmol per gram fresh weight (15- to 23-fold increases
369 relative to wild type).

370 None of the *CYC1*-RNAi lines accumulated detectable levels of loganic acid (**2**) in any
371 tissue and in most tissues, the levels of secologanic acid (**3**), strictosidinic acid (**5**) and the post-
372 strictosidinic acid intermediates were also reduced at least six-fold relative to wild type (Figure 9
373 and Table 3), with strictosamide epoxide (**7**), strictosamide diol (**8**) and strictosamide ketolactam
374 (**9**) levels being reduced to below the detection limit. With regard to the isomer composition of
375 strictosidinic acid (**5**) and post-strictosidinic acid metabolites, the levels of all identified isomers
376 were decreased in *CYC1*-RNAi lines relative to those in wild type, in some tissues to below the
377 detection limit (Table 3). Isomer compositions were also radically altered in certain tissues of the
378 *CYC1*-RNAi lines compared to average wild type levels. For example, strictosidinic acid (**5**) was
379 composed of 39% isomer 2 (21(*S*) isomer) and 61% isomer 3 (21(*R*) isomer) in mature leaves of
380 wild type, whereas in *CYC1*-RNAi lines, isomer 3 was more dominant (94%). Strictosamide (**6**)
381 in roots and stems of wild type consisted mainly of isomer 1 (74% and 87%, respectively), while
382 isomer 2 was exclusively accumulated in *CYC1*-RNAi lines. Pumiloside (**10**) in stems of wild
383 type was composed of 41% isomer 2, whereas in *CYC1*-RNAi lines, pumiloside isomer 1 was the
384 only detectable isomer. Surprisingly, deoxypumiloside (**11**) isomer compositions did not
385 significantly differ between wild type and *CYC1*-RNAi plants. These combined results for the
386 impact of *CYC1*-RNAi are consistent with the metabolite profiles of *TDC1*-RNAi lines and the
387 proposed pathway for camptothecin biosynthesis (Figure 9 and Figure 1).

388

389 **Transcriptional crosstalk between the indole and iridoid biosynthetic pathways**

390

391 To test whether indole and iridoid precursor synthesis might be coordinated, we analyzed
392 the expression of additional candidate genes in RNAi plants compared to wild type. *CYC1*,
393 *CYC2*, and *G8O* (geraniol-8-oxidase, Figure 5) mRNA levels were determined and compared in
394 the roots and green stems of *TDC1*-RNAi and wild type plants (Figure 10). All three genes were

expressed most highly in stems (Figure 10 B and D), with *CYC2* mRNA levels not being significantly different in any genotype or tissue. However, in *TDC1*-RNAi roots, *CYC1* and *G8O* mRNA levels were increased 9-fold and 40-fold, respectively, relative to wild type (Figure 10 A), suggesting that in response to the severe reduction in tryptamine and camptothecin biosynthesis (Figure 9) the monoterpene branch of the pathway is specifically up-regulated in roots of *TDC1*-RNAi plants. *CYC1*-RNAi lines with strong impact on *CYC1* expression and mature leaf camptothecin levels were similarly assessed for *TDC1*, *CYC2* and *G8O* expression (Figure 910 C and D). While *G8O* and *CYC2* transcript levels were not significantly different between *CYC1*-RNAi lines and wild type plants, *TDC1* expression was significantly increased 3-fold in roots (Figure 10 C), suggesting that in response to the severe reduction in levels of monoterpene intermediates (Figure 9 and Table 3) and camptothecin biosynthesis in *CYC1*-RNAi lines, the indole branch is up-regulated. These data indicate the existence of a transcriptional crosstalk mechanism between the indole and the iridoid branch of the camptothecin pathway in *C. acuminata* roots.

DISCUSSION

The *C. acuminata* seco-iridoid pathway generates isomeric, acidic precursors for camptothecin biosynthesis

Our results indicate that *C. acuminata* (order Cornales) uses a seco-iridoid pathway that fundamentally differs from that in *C. roseus* and *R. serpentina,* two plant species in the order Gentianales in which seco-iridoid and MIA synthesis has been most extensively studied (De Luca et al., 2014). *C. roseus* and *R. serpentina* form the methyl esters loganin and secologanin to produce the key MIA precursor strictosidine. These compounds are absent from *C. acuminata* and instead, the carboxylic acids loganic acid (**2**) and secologanic acid (**3**) accumulate and are utilized to synthesize strictosidinic acid (**5**) (Table 1). In this regard, *C. acuminata* also differs from *O. pumila*, the only other camptothecin-producing species for which some biochemical and molecular data exist. Like *C. roseus* and *R. serpentine*, *O. pumila* is also in the order Gentianales and utilizes methyl ester intermediates to produce strictosidine (Asano et al., 2013). Consistent with this, protein extracts from *O. pumila* tissues showed strictosidine synthase activity while

425 those from *C. acuminata* leaves, stems and root tissues lacked this activity (Yamazaki et al.
426 2003). These combined data indicate that at least two routes for camptothecin have evolved in
427 plants, a "Gentianales-type" pathway exemplified by *O. pumila* and a novel pathway in *C.*
428 *acuminata* (Figure 1) that is identical to the "Gentianales-type" seco-iridoid pathway only up
429 through loganic acid formation and thereafter uses carboxylic acid, instead of methyl ester,
430 intermediates (Asano et al., 2013; Miettinen et al., 2014; Salim et al., 2014).

431 In *C. acuminata*, tryptamine (**4**) is condensed with secologanic acid (**3**) to form
432 strictosidinic acid (**5**), instead of with secologanin to form strictosidine as in the order
433 Gentianales. Moreover, plant species of the order Gentianales form a single isomer of
434 strictosidine as the initial MIA intermediate (Asano et al., 2013; Miettinen et al., 2014) while *C.*
435 *acuminata* produces a mixture of strictosidinic acid (**5**) isomers as its initial MIA intermediate
436 (Figures 2 and 3 and Table 3). NMR analyses of the two major strictosidinic acid isomers
437 (isomers 2 and 3) show that they differ in stereochemical configuration (are diastereomers) at
438 position C21, the site of glucosylation (Figure 3, Table 2). These data suggest that all iridoids in
439 the pathway leading to strictosidinic acid are also present as isomeric mixtures. Prior to
440 glucosylation, equilibrium between the open-ring and closed-ring conformations of 7-
441 deoxyloganetic acid yields stereoisomers at the C2 carbon atom (Figure 4), both of which are
442 subsequently glucosylated (Figure 1). This proposed mechanism is consistent with the detection
443 of two isomers for loganic acid (**2**) and secologanic acid (**3**) (Supplemental Figure S1 and
444 Supplemental Figure S2) as well as the presence of isomer mixtures for strictosidinic acid (**5**)
445 and most post-strictosidinic acid intermediates (Table 1).

446 Silencing of two essential genes for synthesis of the monoterpene and indole components
447 of camptothecin, *CYC1* and *TDC1*, respectively, provide strong evidence for the involvement of
448 specific metabolites in the proposed camptothecin pathway in *C. acuminata*. *CYC1* RNAi lines
449 with low *CYC1* transcript levels had levels of the iridoid loganic acid reduced to below detection
450 and significantly lowered levels of secologanic acid compared to wild type (Figure 9).
451 Additionally, the levels and isomers of all strictosidinic acid (**5**) and post-strictosidinic acid
452 intermediates (including camptothecin) were significantly decreased in *CYC1*-RNAi lines
453 relative to wild type (Figure 9 and Table 3). These data are consistent with the iridoid synthase
454 activity of CYC1 *in vitro* (Figure 6) and with CYC1 being the major, and possibly only, iridoid

synthase involved in camptothecin synthesis in *C. acuminata*. Silencing of *TDC1* greatly impaired the plants' production of tryptamine (**4**) and all indole-containing intermediates/isomers of the proposed camptothecin pathway (Figure 9). Additional evidence for the indole-dependent synthesis of various strictosidinic acid (**5**) and post-strictosidinic acid isomers was obtained by feeding experiments with *TDC1*-RNAi apical cuttings, where deuterated tryptamine was incorporated into many of the proposed intermediates and their isomers, including camptothecin (Table 1). Most significantly, *TDC1*-RNAi and *CYC1*-RNAi lines impacted, to different degrees, the same strictosidinic acid (**5**) and post-strictosidinic acid intermediates/isomers.

Combining non-targeted metabolite analyses in wild type with metabolite profiling in RNAi lines allowed us to identify new pathway intermediates of extremely low abundance in wild type (i.e., strictosamide epoxide, diol and ketolactam) that are consistent with the biosynthetic scheme shown in Figure 1. These three novel metabolites are likely formed from isomeric strictosamide (**6**) yielding first strictosamide epoxide (**7**) that is further converted to strictosamide diol (**8**) and then to its ketolactam (**9**), which undergoes intramolecular cyclization of enolate to carbonyl, followed by dehydration, in a manner similar to the well-known aldol condensation. This process channels strictosamide (**6**) towards pumiloside (**10**) synthesis by completing the quinolone ring topology that provides the framework for camptothecin. In the proposed pathway, pumiloside isomers are then reduced to deoxypumiloside (**11**) isomers. Although the sequential order of subsequent metabolic conversions that resolve the diastereomers at carbon-21 to the single stereochemistry in camptothecin has not been established, it is evident from the chemistry that de-glucosylation and oxidations are involved. After de-glucosylation, these final reactions convert the chiral sp^3 carbon-21 to a sp^2 carbon and eliminate the chirality at the C-atom site of glucosylation. Notably, de-glucosylation of *R* and *S* diastereomers leads to formation of an aglucone whose ring can again spontaneously open and close, just as in non-glucosylated iridoids (Figure 1 and Figure 4). Later oxidation of the ring C-atom to a carbonyl C-atom "fixes" the closed ring conformation and hence, determines the single stereochemistry present in camptothecin.

The abundance of glucoside isomer mixtures for the majority of the camptothecin biosynthetic pathway, from loganic acid (**2**) to deoxypumiloside (**11**), is both remarkable and unprecedented in MIA biosynthesis. This has profound implications from a mechanistic

perspective because it suggests that some, if not all, of the enzymes from 7-deoxyloganetic acid to deoxypumiloside (**11**) are able to accommodate multiple isomers or that multiple enzymes exist for each step that are specific for a single stereoisomer. Given that the metabolic transformations from strictosidinic acid (**5**) to deoxypumiloside (**11**) are remote from the site of glycosylation, the consistent presence of multiple intermediate isomers in this portion of the pathway suggests that a single enzyme could accommodate both stereoisomer substrates. However, the variation in the isomeric composition of strictosidinic acid (**5**) and post-strictosidinic acid compounds between different tissues in wild type as well as the marked changes in the isomer composition of certain metabolites in some *CYC1*-RNAi tissues (Table 3) indicate that additional stereo-selective sinks or processes are active in *C. acuminata*.

Genetic evidence for the alternative seco-iridoid pathway in *C. acuminata*

Besides CYC1, additional candidates for the early steps of the *C. acuminata* seco-iridoid pathway formed a tight 23 transcript "seco-iridoid" cluster in transcriptome-wide co-expression analyses (Figure 5). This cluster includes transcripts encoding proteins with high sequence identities (65-78%) to *C. roseus* geraniol synthase (Kumar et al. 2015), G8O (Hofer et al. 2013), CYC1 (Geu-Flores et al. 2012), 7-deoxyloganetic acid synthase (Salim et al., 2014) and glucosyltransferase (Asada et al., 2013) (Figure 5) and BIS1, a bHLH transcription factor that regulates iridoid synthesis in *C. roseus*. CYC2 is also in this cluster but is not likely to be involved in camptothecin biosynthesis as it lacks iridoid synthase activity *in vitro* (Figure 5) and, despite still being coordinately expressed with CYC1, was unable to compensate for loss of CYC1 activity in *CYC1*-RNAi lines (Figures 9 and 10). This cluster also included two transcripts encoding proteins that could conceivably contribute to iridoid and/or camptothecin production in *C. acuminata*, an aldo/keto reductase and protein S, an α/β-hydrolase superfamily protein associated with MIA synthesizing cells in *C. roseus* (Leménager et al., 2005). With the exception of a CYP76A1 transcript, other transcripts are genes of unknown function or homologous to proteins inconsistent with a role in the pathway. Finally, in contrast to the high identity of early iridoid pathway enzymes in *C. acuminata* and *C. roseus*, the last two steps of the seco-iridoid pathway in *C. roseus*, secologanin synthase (a P450) and strictosidine synthase lack obvious orthologs in the *C. acuminata* transcriptome (several transcripts with approximately

50% and 37% identities, respectively, Supplemental Data Set S2). These low identities may be a reflection of their different substrates in the two species: *C. acuminata* enzymes using ionizable, carboxylic acid intermediates while *C. roseus* substrates are the equivalent non-ionizable methyl esters. The fact that none of these low identity secologanin and strictosidine synthase candidates are present in the "seco-iridoid" cluster suggests the latter portion of seco-iridoid synthesis in *C. acuminata* is at minimum not co-regulated with its earlier steps. This is likely also true for post-strictosidinic acid steps of the pathway as, with the exception of a CYP76A1 and an aldo/keto reductase, the "seco-iridoid" cluster also lacks additional transcripts predicted to encode the reductases, oxidases or glucosidases postulated to carry out post-strictosidinic acid steps (see Figure 1).

The extreme diversity of monoterpene indole alkaloids in nature raises fundamental questions about evolution of the pathway, especially in light of the data presented here for *C. acuminata*. Synthesis of loganic acid has been documented for numerous other plant species from unrelated plant orders and families (Skaltsounis et al. 1989, Mueller et al. 1998, Rastrelli et al. 1998, Graikou et al. 2002, Han et al. 2008, Serrilli et al. 2008, Aberham et al. 2011, Zhang et al. 2012, Asano et al. 2013, Zhou et al. 2013, Fan et al. 2014) and it appears to represent a trait that arose relatively early in plant evolution. The highly conserved proteins for early seco-iridoid biosynthesis in the unrelated species *C. acuminata* and *C. roseus* are consistent with this interpretation. By contrast, the differences in seco-iridoid biosynthesis that yield exclusively strictosidinic acid in *C. acuminata* (Cornales) and strictosidine in the Gentianales (*C. roseus*, *R. serpentina* and *O. pumila*) indicate that post-loganic acid steps likely evolved later. In this context, it must be mentioned that although *C. roseus*, *R. serpentina* and *O. pumila* all produce exclusively strictosidine, several other members of the Gentianales, most notably other *Ophiorrhiza* species, are able to produce strictosidinic acid (Arbain et al. 1993, Hamzah et al. 1994, Reanmongkol et al. 2000, Cardoso et al. 2004, Atsuko et al. 2008, Olusegun et al. 2011, Farias et al. 2012). As additional biochemical and genetic information is not available for these strictosidinic acid producing Gentianales, a comparison of them with *C. roseus* and *C. acuminata* is not possible but would help clarify if strictosidinic acid arose independently (i.e., by convergent evolution) or whether the lack of secologanic acid methylation in *C. acuminata* is an ancestral trait.

545

546 **Where is camptothecin biosynthesis located in *C. acuminata*?**

547 The compartmentalization of alkaloid biosynthesis is remarkably diverse and complex
548 across the plant kingdom with various studies demonstrating localization of distinct steps to
549 specific organelles, cell types, tissues and organs (Ziegler and Facchini 2008, Courdavault et al.
550 2014, De Luca et al. 2014, Bedewitz et al. 2014). In this regard, it is apparent from expression
551 profiles (Figures 5 and 10 and Supplemental Data Set S3) that *TDC1* and *CYC1* and other early
552 seco-iridoid candidate genes are expressed most highly in stems and roots of wild-type *C.*
553 *acuminata*, suggesting these two tissues are particularly important sites for synthesis of indole
554 and seco-iridoid precursors. Indeed, wild-type stems exhibited the highest *TDC1*, *G8O,* and
555 *CYC1* transcript levels (Figures 8 and 10) and high levels of tryptamine, loganic acid and
556 secologanic acid (Figure 2). Stems were also the only wild-type tissue that contained detectable
557 levels of all the metabolites and isomers reported in this study, including the low abundance
558 intermediates strictosamide epoxide (**7**), diol (**8**) and ketolactam (**9**), which is consistent with
559 stem playing a key role in the synthesis of post-strictosidinic acid metabolites. Finally, in labeled
560 tryptamine feeding experiments, *TDC1*-RNAi stems accumulated the largest number of labeled
561 metabolites, including camptothecin, further supporting a key role for this tissue in the synthesis
562 and/or transport of metabolites involved in camptothecin synthesis.

563 Gene expression and metabolite analyses in roots of RNAi lines suggested the presence
564 of one or more regulatory system influencing and balancing the production of indole and seco-
565 iridoid precursors for MIA synthesis (Figure 9 and Figure 10). Roots were the only tissue that
566 specifically up-regulated expression of the seco-iridoid genes *CYC1* and *G8O* in *TDC1*-RNAi
567 plants (leading to accumulation of loganic acid (**2**)) and up-regulated expression of *TDC1* in
568 *CYC1*-RNAi (leading to accumulation of tryptamine (**4**)). These data suggest a transcriptional
569 regulatory mechanism that enhances flux of precursors from the indole and iridoid branches in
570 roots, likely in response to cellular signals, indicating MIA synthesis is below a desired level.
571 Such a system would permit *C. acuminata* to balance the production of indole and seco-iridoid
572 precursors for export to aerial tissues or for use in maintaining a constitutive level of MIAs for
573 defense against herbivore attack of roots. The simultaneous up-regulation of *G8O* and *CYC1* in
574 *TDC1*-RNAi roots (Figure 10 A) and their clustering in co-expression analyses (Figure 5) with

other seco-iridoid pathway candidates, including a putative ortholog of the *C. roseus* iridoid transcription factor BIS1, indicates that the pathway up to loganic acid synthesis is tightly co-regulated. It seems plausible that in response to MIA deficiency in *TDC1*-RNAi roots that BIS1 or other transcription factors are impacted and mediate the observed effects on iridoid pathway transcripts. In transcriptome-wide co-expression analysis, *TDC1* and the seco-iridoid pathway genes were in separate clusters (Figure 5), indicating that the two branches are regulated in distinct ways. This is reinforced in targeted coexpression analyses using only transcripts from the seco-iridoid cluster in Figure 5 and MEP and tryptophan pathway enzymes, which provide IPP and tryptophan for iridoid and tryptamine synthesis. With few exceptions, transcripts from the three biochemical pathways cluster within their respective biosynthetic groups. Transcriptome analysis of various tissues from the RNAi lines is needed to gain a deeper understanding of the coordinated control of the tryptamine and iridoid branches in *C. acuminata.*

MATERIAL AND METHODS

Transcriptome resources and computational analyses

The transcriptome profile for 53,154 unique *C. acuminata* transcripts was downloaded from the MPGR database where expression abundances are represented as fragments per kilobase of transcript per million mapped reads (FPKM) (ftp://ftp.plantbiology.msu.edu/pub/data/MPGR/Camptotheca_acuminata/, (Gongora-Castillo et al., 2012)). The RNA-seq reads are available in the NCBI SRA under accession number SRP006330. Co-expression analyses were performed with the Multi-experiment Viewer software package (MeV v4.9) (Saeed et al., 2006) using $\log_2$-transformed FPKM expression values. Candidate genes identified in the present study and their respective MPGR sequence numbers are given in Figure 5 and Supplemental Data Set S2.

To analyze the phylogenetic relationship of progesterone 5-beta-reductase family members, the protein sequences for *C. acuminata* and *R. serpentina* were derived from the following transcript sequences at http://medicinalplantgenomics.msu.edu and *C. roseus*

605 sequences were searched in GenBank: ***C. roseus*:** KJ873882 (CrP5bR1), KJ873883 (CrP5bR2),
606 KJ873884 (CrP5bR3), KJ873885 (CrP5bR4), KJ873886 (CrP5bR5, iridoid synthase), KJ873887
607 (CrP5bR6); ***C. acuminata*:** KU842378 (CYC1), KU842379 (CYC2), GACF01077314,
608 GACF01008548, GACF01024182, GACF01073333, GACF01036291; and ***R. serpentina*:**
609 GACE01080250, GACE01016867, GACE01082242, GACE01021747, GACE01073438,
610 GACE01070053, GACE01001096 and GACE01023577. Protein sequences were aligned with
611 ClustalW. A neighbor-joining tree was constructed with MEGA 6.06 (Tamura et al. 2011). The
612 complete deletion option was used and bootstrap values determined from 1,000 replicates and
613 evolutionary distances computed using the Poisson correction method (Supplemental Figure S4;
614 Supplemental Data Set S4).
615
616 **Amplification of the coding sequences for TDC1 and putative iridoid synthases from *C.***
617 ***acuminata***
618 The open reading frames for *TDC1* and the putative iridoid synthases, *CYC1* and *CYC2*,
619 were amplified by PCR with sequence-specific primers (Supplemental Table S2) from *C.*
620 *acuminata* cDNA and the amplicons were then inserted into pENTR-SD/D (Life Technologies).
621 The identities of the cloned fragments for *TDC1* (1513 bp), *CYC1* (1174 bp) and *CYC2* (1198
622 bp) were confirmed by sequencing.
623
624 **Heterologous expression and purification of recombinant proteins**
625 The full-length CYC1 and CYC2 coding sequences were cloned into the pDEST17
626 expression vector (Life Technologies). The *C. roseus* iridoid synthase (Geu-Flores et al., 2012)
627 was also cloned into pDEST17. *Escherichia coli* Rosetta (DE3) cells harboring the pDEST17
628 constructs were grown at 37°C. Heterologous expression was induced with 0.5 mM isopropyl β-
629 D-thiogalactopyranoside at an OD_{600nm} of 0.8. Cultures were then incubated at 16°C and cells
630 were harvested after 8 h or 16 h and lysed. The crude cell lysates were centrifuged at 20,000 × g
631 and the His-tagged proteins in the supernatants were purified by Ni-chelating chromatography
632 following manufacturer's instructions (Qiagen). The protein extracts were concentrated and the
633 buffer was exchanged to 50 mM MOPS pH 7.0 before storage at -80°C.
634

635 **Dehydrogenase activity and iridoid synthase assays**

636 Purified proteins were assayed for NAD(P)H dependent dehydrogenase activity using
637 nitroblue tetrazolium (NBT) chloride as electron acceptor, which when reduced, forms a dark
638 blue formazan precipitate (Chigri et al., 2006). A 50-µl reaction mixture contained up to 4 µg
639 protein, 200 µM NAD(P)H and 80 µg NBT in 50 mM Tris HCl pH 7.8. Control reactions were
640 carried out lacking NAD(P)H or protein.

641 8-Oxogeranial (**1**) was the generous gift of Drs. Sarah E. O´Connor and Nat Sherden
642 (John Innes Centre, UK) and was synthesized from geraniol according to (Geu-Flores et al.,
643 2012) and contained a mixture of the two isomers 8-oxogeranial (**1**) and 8-oxoneral in an
644 approximate ratio of 2:1. Reaction mixtures (100 µL total volume) contained 2.5 µg protein, 400
645 µM monoterpene substrate(s) and 400 µM NAD(P)H in 20 mM MOPS (pH 7.0) and were
646 incubated for 1 h at room temperature. Assays were terminated and extracted with 200 µL
647 dichloromethane. The reaction products were separated and analyzed by GC-MS in an Agilent
648 6890N system coupled to an Agilent 5973 MS detector. Chromatography was performed with an
649 Agilent VF-5ms column (30 m × 0.25 mm × 0.25 µm plus 10 m EZ-Guard; part #CP9013) at 1.2
650 ml min^{-1} helium flow. The injection volume was 1 µL in split-less mode at an injector
651 temperature of 250°C. The following oven program was used (run time 16.01 min): 1 min
652 isothermal at 50°C, 20°C min^{-1} to 150°C, 45°C min^{-1} to 280°C, 4 min isothermal at 280°C, 40°C
653 min^{-1} to 325°C and 2 min isothermal at 325°C. The mass spectrometer was operated using 70 eV
654 electron ionization (EI) mode with the following settings: solvent delay 2 min, resulting EM
655 voltage 2141.2, ion source temperature at 230°C and quadrupole temperature at 150°C. Mass
656 spectra were recorded from *m/z* 30 to 600 at 3 spectra/s.

657

658 **Cloning and construction of pHellsgate constructs**

659 To suppress expression of *TDC1* or *CYC1* in *C. acuminata*, 442-bp and 363-bp cDNA
660 sequences, respectively, were amplified by PCR from the cloned full-length coding sequences.
661 The amplicons were cloned into pENTR-D (Life Technologies) and then inserted into the binary
662 vector pHellsgate12 (Helliwell and Waterhouse, 2005) and verified by restriction analyses and
663 sequencing. The constructs were then transformed into *A. tumefaciens* strain EHA105 (Hellens et
664 al., 2000).

665

666 ***C. acuminata* cultivation and generation of transgenic RNAi lines**

667 Mature *C. acuminata* seeds were collected from trees growing in the San Antonio Zoo
668 (Texas, USA). De-husked seeds were cleaned with 0.5% Tween 20 for at least 30 minutes, rinsed
669 4-5 times with distilled water and then planted on 96-well flats with Redi-Earth Plug & Seedling
670 Mix (Hummert International). Flats were kept in a growth room at 25°C ± 2°C under a 16-h
671 photoperiod (100 µmol $m^{-2}s^{-1}$). Cotyledons from 3-week-old seedlings were used for *A.*
672 *tumefaciens*-mediated transformation with RNAi expression constructs. Seedlings were surface-
673 sterilized using a 10% commercial bleach solution containing 0.1% Tween 20 for 10 minutes,
674 then rinsed four times with sterile distilled water.

675 *A. tumefaciens* EHA105 clones harboring a pHellsgate 12 construct were grown
676 overnight at 28°C in Luria Bertani (LB) medium containing 25 µg/ml rifampicin and 50 µg/ml
677 kanamycin. For infection, an *A. tumefaciens* suspension (OD_{600nm} of 0.6) was made from an
678 overnight culture using Lloyd & McCown liquid medium containing 100 µM acetosyringone.
679 Prior to transformation, cotyledon sections were excised and pre-cultured for 3 days in callus
680 induction media (WPM Lloyd & McCown with vitamins) (Lloyd, 1981), 2% sucrose, 2 mg/L 1-
681 naphthalene acetic acid (NAA) and 2 mg/L 6-benzylaminopurine (BAP), pH 5.8 and 0.8 % agar).
682 Pre-cultured explants were submerged in the *A. tumefaciens* inoculum for 5 minutes, and then
683 transferred to fresh agar plates for two days at 25°C in the dark. Cotyledons were then
684 transferred to fresh callus induction media supplemented with 500 mg/L carbenicillin and 100
685 mg/L cefotaxime for 6-7 days at 25°C ± 2°C under a 16-h photoperiod (70 µmol.m^{-2}.s^{-1}).

686 For selection of transformants, inoculated cotyledon explants were transferred to shoot
687 induction and proliferation media WPM Lloyd & McCown (Lloyd, 1981) supplemented with 2%
688 sucrose, 1 mg/L BAP, 0.3 mg/L indole-3-butyric acid (IBA), 500 mg/L carbenicillin, 100 mg/L
689 cefotaxime and 30 mg/L kanamycin. Subculture of explants to the same medium was performed
690 every 2-3 weeks. Kanamycin-resistant shoots were excised and transferred to shoot elongation
691 media (WPM Lloyd & McCown supplemented with 3% sucrose, 0.15 mg/L gibberellic acid
692 (GA3), 0.15 mg/L BAP, 500 mg/L carbenicillin, 100 mg/L cefotaxime and 30 mg/L kanamycin).
693 Elongated shoots were rooted using shoot induction media supplemented with 1 mg/L IBA.
694 Plantlets with roots were then transferred to pots containing RediEarth soil mix and allowed to

acclimate at 25°C ± 2°C under a 16-h photoperiod (100 μmol.m^{-2}.s^{-1}) for several weeks prior to transfer to greenhouse for further cultivation.

Real-Time Quantitative RT-PCR

Total RNA was extracted from 100 mg *C. acuminata* tissue by the hot-borate protocol (Birtic and Kranner, 2006). Prior to cDNA synthesis, the RNA extracts were treated with TURBO DNase (Ambion) to remove residual genomic DNA. cDNAs were synthesized from 1 μg of total RNA using SuperScript II Reverse Transcriptase (Life Technologies) and Oligo(dT)$_{18}$ primer. qRT-PCRs were performed in triplicate in a Mastercycler RealPlex 2 (Eppendorf). Each 20-μl reaction contained 1x SYBR Green PCR Master Mix (Life Technologies, Applied Biosystems), forward and reverse primers (Supplemental Table S2) at a final concentration of 0.5 μM and 2 μl of 1:4 diluted *C. acuminata* cDNA. The following temperature profile was used for qRT-PCR analyses: 10 min at 95°C followed by 40 cycles with 15 s at 95°C and 1 min at 60°C. Single fragment amplification was verified by gel electrophoresis on a 3% agarose gel and visualization of the ethidium bromide stained DNA under UV light as well as by sequence analyses of PCR products from selected samples. Ct values were normalized to *ACTIN6*.

Metabolite analyses in *C. acuminata* non-transgenic and transgenic lines

For each sample, approximately 30 mg of frozen powdered plant tissue and 500 μl acetonitrile/water (7/3, v/v) containing 1.25 μM telmisartan (internal standard) was added, vortexed for 5 s and incubated in the dark at 4°C for 16 h. Samples were then centrifuged at 4°C and 10,000 × g for 30 min, supernatants were transferred to fresh tubes and centrifuged at 4°C and 10,000 × g for 15 min, and 40-μl aliquots were diluted by addition of 150 μl deionized water. Immediately prior to UHPLC/MS analysis, 10 μl of 10% formic acid was added by the autosampler to each extract and mixed by drawing the liquid into the autosampler syringe and ejecting back into the sample vial. This procedure minimized acid-catalyzed degradation while vials remained in the autosampler tray, and delivered metabolites to the column in an acidic solvent that improved chromatographic retention and resolution. Individual standard solutions of available standards tryptamine, loganic acid (ChromaDex), camptothecin (MP Biomedicals, LLC) and the internal standard telmisartan (Toronto Research Chemicals) were prepared over a

725 range of concentrations from 0 - 70 μM, and were analyzed together with each set of plant tissue
726 extracts. Typical limits of detection were about 0.1 μM for each analyte, with a linear response
727 of up to at least 50 μM in each case. UHPLC/MS analyses were performed using a Shimadzu
728 LC-20AD ternary pump coupled to a SIL-5000 autosampler, column oven, and Waters LCT
729 Premier mass spectrometer equipped with an electrospray ionization source. A 10-μL volume of
730 each extract was analyzed using either a 52-min or a 15-min gradient elution method on an
731 Ascentis Express C18 UHPLC column (2.1 × 100 mm, 2.7 μm) with mobile phases consisting of
732 10 mM ammonium formate in water, adjusted to pH 2.85 with formic acid (solvent A) and
733 methanol (solvent B). The 52-min method gradient was as follows: 2% B at 0.00-2.00 min, linear
734 gradient to 20% B at 20.00 min, linear gradient to 55% B at 43.00 min, then a step to 99% B at
735 43.01 min, then return to 2% B over 47.01-52.00 min. The 15-min method employed 8% B at
736 0.00-1.00 min, linear gradient to 40% B at 3.00 min, linear gradient to 70% B at 11.00 min, then
737 step to 99% B at 11.01 and held until 13.00 min, followed by a return to 8% B and held from
738 14.00-15.00 min. For both gradients, the flow rate was 0.3 ml/min and the column temperature
739 was 45°C. The mass spectrometer was operated using V optics in positive-ion mode with a
740 typical resolution of ~ 4000 at full width at half maximum. Source parameters were as follows:
741 capillary voltage 3200 V, sample cone voltage 10 V, desolvation temperature 350°C, source
742 temperature 100°C, cone gas flow 40 L/h and desolvation gas flow 350 L/h. Mass spectrum
743 acquisition was performed in positive-ion mode over *m/z* 50 to 1,500 with scan time of 0.1 s,
744 using dynamic range extension. Mass spectra containing fragment ions were generated by rapid
745 switching of aperture 1 voltage over four parallel data acquisition functions (20, 40, 60 and 80 V)
746 (Gu et al., 2010). The lowest aperture 1 voltage yielded negligible in-source fragmentation for all
747 metabolites except the iridoid glycosides loganic acid and secologanic acid, which, in addition to
748 $[M+H]^+$ and $[M+\text{alkali metal}]^+$ ions, also yielded ions corresponding to neutral loss of the
749 glucose moiety (162 Da). Accurate masses and fragments were confirmed in UHPLC/MS/MS
750 analyses (Xevo G2-S and G2-XS QTOF mass spectrometers, Waters) by using four scan
751 functions (method A: 10, 20, 40 and 60 V) or a collision energy ramp (method B, from 10-50 V
752 for *m/z* 200 to 15-80 V at *m/z* 1000) (Table 1 and Supplemental Table 1).
753 For quantitative analyses, the 15-min gradient UHPLC/MS method was used. The
754 extracted ion chromatograms for each target analyte were integrated, and analytes were

755 quantified, using QuanLynx tool (Waters) with a mass window allowance of 0.2. Sodium adduct
756 peaks $[M+Na]^+$ and $[M+H]^+$ were quantified for carboxylic acids and downstream metabolites,
757 respectively. All calculated peak areas were normalized to the peak area for the internal standard
758 telmisartan and tissue fresh weight.
759 Separation of loganic acid and secologanic acid isomers was obtained by using a 31-min
760 gradient elution method on an Agilent ZORBAX Eclipse XDB C8 HPLC column (4.6 × 150
761 mm, 5 µm) with mobile phases consisting of 0.1% v/v formic acid in water (solvent A) and
762 acetonitrile (solvent B). The elution gradient was: 5% B at 0.00-1.00 min, linear increase to 10%
763 B at 3.00 min, linear to 30% B at 25.00 min, followed by a rapid increase from 30-99% B over
764 25.00-26.00 min, hold at 99% B over 26.01-28.00 min, then return to 5% B and held over 29.00-
765 31.00 min. The flow rate was 1.0 ml/min and the column temperature was 30°C. Loganic acid
766 isomer 1, loganic acid isomer 2, secologanic acid isomer 1 and isomer 2 eluted at 5.2 min, 6.1
767 min, 8.2 min and 8.6 min, respectively.
768
769 **NMR characterization of strictosidinic acid isomers**
770 Young leaf tissue (350 g fresh weight) was freshly harvested from greenhouse-cultivated
771 *C. acuminata* plants, transferred to a 4 L amber glass bottle, and extracted using 2 L of HPLC
772 grade acetonitrile for 16 h at 4°C. The extract was ultrasonicated for 2 minutes followed by
773 liquid-liquid partitioning against two volumes of 500 mL hexane. The lower acetonitrile layer
774 was collected, and solvent was removed under reduced pressure in a rotary evaporator and
775 reconstituted in 10 mL of methanol/water (5/95 v/v) immediately before UHPLC/MS metabolite
776 profiling. UHPLC/MS metabolite profiling was performed using a Shimadzu LC-20AD ternary
777 pump coupled to a SIL-5000 autosampler, column oven, and Waters LCT Premier mass
778 spectrometer equipped with an electrospray ionization source and operated in positive-ion mode.
779 Preparative HPLC fractionation was performed using a Waters Model 2795 HPLC system
780 coupled to a LKB BROMMA 221 fraction collector. An Ascentis Express F5
781 (pentafluorophenylpropyl) column (4.6 x 150 mm, 2.7 µm particles; Supelco Sigma-Aldrich)
782 was used with a solvent flow rate of 0.8 mL/min for profiling and preparative fractionation. The
783 flow was split post-column, and approximately 0.3 mL/min was diverted to the mass
784 spectrometer. The mobile phase consisted of water (Solvent A) and methanol (Solvent B) using

785 linear gradients: 10% B during 0-1 min, to 30% B at 2 min, to 50% B at 14 min, to 65% B at 15
786 min, to 90% B at 25 min, then 90-99% B over 25-32 min followed by a hold until 36 min, then
787 return to 10% B over 36.01-40 min. Fractions were collected at 15-s intervals, and 50 injections
788 of 150 µL were made to accumulate sufficient material for NMR analysis. Two major
789 strictosidinic acid isomers, denoted isomers 2 and 3 based on the order of their elution times on
790 the C18 column, were collected in fractions 60-66 and 42-46, respectively from the F5 column.
791 Fractions for each isomer were combined, dried under reduced pressure and reconstituted in
792 CD_3OD. NMR spectra (^1H, J-resolved ^1H, ^1H-^1H COSY, HSQC, cHSQC, HMBC) were recorded
793 on a 21.1 T Bruker Avance-900 NMR spectrometer equipped with a TCI inverse triple-resonance
794 cryoprobe at 900 MHz (^1H) and 225 MHz (^{13}C) at the Michigan State University Max T. Rogers
795 NMR Facility. Additional NMR data are presented in Supplemental Table S3 and Supplemental
796 Data Set S1.
797
798 **In vivo labeling studies of *C. acuminata* apical cuttings**
799 Shoot cuttings of approximately twenty centimeters in length were taken from
800 approximately 1-year-old wild type and *TDC1*-RNAi plants. Shoots were incubated individually
801 in 15 ml conical tubes containing 100 µM [α,α,β,β-d_4]-tryptamine (CDN Isotopes, 97% isotopic
802 enrichment) and 10-15 mg carbenicillin in 10 ml water at room temperature under continuous
803 light (25 $\mu mol.m^{-2}.s^{-1}$). Controls were similarly treated without addition of deuterated tryptamine.
804 Six biological replicates were performed for each treatment. The water level was regularly
805 adjusted with water or 100 µM deuterated tryptamine solution as needed. After six weeks, stems
806 and leaves were harvested separately, frozen with liquid nitrogen and analyzed as described
807 above using the 52-min UHPLC/MS method.
808
809 **ACCESSION NUMBERS**
810 *C. acuminata* sequence data from this article can be found in the GenBank/EMBL data libraries
811 under the following accession numbers: KU842377 (*TDC1*), KU842378 (*CYC1*, iridoid
812 synthase) and KU842379 (*CYC2*, progesterone 5-beta reductase like). All MPGR sequence data
813 were previously deposited in GenBank (Gongora-Castillo et al. 2012) and relevant accession
814 numbers are listed in Supplemental Data Set S2.

SUPPLEMENTAL DATA

Supplemental Figure S1. Loganic acid isomers in *C. acuminata*.

Supplemental Figure S2. Secologanic acid isomers in *C. acuminata*.

Supplemental Figure S3. Heat map of expression data for candidate genes in the tryptamine and seco-iridoid branch of the camptothecin pathway.

Supplemental Figure S4. Phylogenetic relationship of progesterone 5-beta-reductase family members from *C. acuminata*, *C. roseus* and *R. serpentina*.

Supplemental Figure S5. Colorimetric dehydrogenase assay with the purified recombinant proteins CYC1, CYC2 and *C. roseus* iridoid synthase.

Supplemental Figure S6. *C. acuminata* wild type (WT) and two RNAi lines.

Supplemental Table S1. Relevant compounds detected in wild-type *C. acuminata*.

Supplemental Table S2. List of primers used in this study.

Supplemental Table S3. NMR Metadata.

Supplemental Data Set S1. NMR spectra.

Supplemental Data Set S2. Accession numbers and sequence identities of *C. acuminata* candidate genes involved in the synthesis of indole and monoterpene components.

Supplemental Data Set S3. FPKM values.

Supplemental Data Set S4. Alignment of the amino acid sequences of progesterone 5-beta-reductase family members from *C. acuminata*, *C. roseus* and *R. serpentina*.

ACKNOWLEDGEMENTS

We thank Sarah E. O´Connor and Nat Sherden (John Innes Centre, UK) for sharing the *C. roseus* iridoid synthase expression construct and 8-oxogeranial, Thomas McKnight (Texas A&M University) for providing us with *C. acuminata* seeds collected from trees at the San Antonio Zoo and Evan Klug and Alexandra Palmiter for technical assistance. Tandem mass spectra were collected using the Waters QTof instruments at the Michigan State University Mass Spectrometry and Metabolomics Core. A.D.J. acknowledges support from Michigan AgBioResearch project MICL-02143 and D.D.P. and A.D.J. from the National Institute of General Medical Sciences project 1RC2GM092521.

AUTHOR CONTRIBUTIONS

R.S., D.D.P. and A.D.J. designed the research; R.S., M.M.-L., S.P., V.S. and A.M. performed the research; R.S., S.P. and V.S. analyzed data. R.S., D.D.P. and A.D.J. wrote the article.

REFERENCES

Aberham, A., Pieri, V., Croom, E.M. Jr, Ellmerer, E., and Stuppner, H. (2011) Analysis of iridoids, secoiridoids and xanthones in *Centaurium erythraea*, *Frasera caroliniensis* and *Gentiana lutea* using LC-MS and RP-HPLC. J. Pharm. Biomed. Anal. 54, 517-525.

Aimi, N., Nishimura, M., Miwa, A., Hoshino, H., Sakai, S., and Haginiwa, J. (1989). Pumiloside and deoxypumiloside; plausible intermediate of camptothecin biosynthesis. Tetrahedron Lett. 30, 4991-4994.

Ajala, O.S., Piggott, A.M., Plisson, F., Khalil, Z., Huang, X., Adesegun, S.A., Coker, H.A.B. and Capon, R.J. (2011) Ikirydinium A: a new indole alkaloid from the seeds of *Hunteria umbellata* (K. Schum). Tetrahedron Lett. 52, 7125-7127.

Arbain, D., Putra, D.P., and Sargent. M.V. (1993) The Alkaloids of *Ophiorrhiza filistipula*. Australian J. Chem. 46(7) 977 – 985.

Asada, K., Salim, V., Masada-Atsumi, S., Edmunds, E., Nagatoshi, M., Terasaka, K., Mizukami, H., and De Luca, V. (2013). A 7-deoxyloganetic acid glucosyltransferase contributes a key step in secologanin biosynthesis in Madagascar periwinkle. Plant Cell 25, 4123-4134.

Asano, T., Kobayashi, K., Kashihara, E., Sudo, H., Sasaki, R., Iijima, Y., Aoki, K., Shibata, D., Saito, K., and Yamazaki, M. (2013). Suppression of camptothecin biosynthetic genes results in metabolic modification of secondary products in hairy roots of *Ophiorrhiza pumila*. Phytochemistry 91, 128-139.

Banerjee, A., and Sharkey, T.D. (2014). Methylerythritol 4-phosphate (MEP) pathway metabolic regulation. Nat. Prod Rep. 31, 1043-1055. Review.

Bedewitz, M.A., Gongora-Castillo, E., Uebler, J.B., Gonzales-Vigil, E., Wiegert-Rininger, K.E., Childs, K.L., Hamilton, .P., Vaillancourt, B., Yeo, Y.S., Chappell, J., DellaPenna, D., Jones, A.D., Buell, C. R. and Barry, C. S. (2014) A root-expressed L-phenylalanine:4-hydroxyphenylpyruvate aminotransferase is required for tropane alkaloid biosynthesis in *Atropa belladonna*. Plant Cell 26, 3745-3762.

Birtic, S., and Kranner, I. (2006). Isolation of high-quality RNA from polyphenol-, polysaccharide- and lipid-rich seeds. Phytochem. Anal. 17, 144-148.

884 Bracher, D., and Kutchan, T.M. (1992). Strictosidine synthase from *Rauvolfia serpentina*:
885 analysis of a gene involved in indole alkaloid biosynthesis. Arch. Biochem. Biophys.
886 294, 717-723.
887 Cardoso, C.L., Castro-Gamboa, I., Silva, D.H., Furlan, M., Epifanio Rde, A., Pinto Ada, C.,
888 Moraes de Rezende, C., Lima, J.A., and Bolzani Vda, S. (2004) Indole glucoalkaloids
889 from *Chimarrhis turbinata* and their evaluation as antioxidant agents and
890 acetylcholinesterase inhibitors. J. Nat. Prod. 67, 1882-1885.
891 Carte, B.K., DeBrosse, C., Eggleston, D., Hemling, M., Mentzer, M., Poehland, B., Troupe, N.,
892 Westley, J.W., and Hecht, S.M. (1990). Isolation and characterization of a presumed
893 biosynthetic precursor of camptothecin from extracts of *Camptotheca acuminata*.
894 Tetrahedron 46, 2747-2760.
895 Chigri, F., Hörmann, F., Stamp, A., Stammers, D.K., Bölter, B., Soll, J., and Vothknecht, U.C.
896 (2006). Calcium regulation of chloroplast protein translocation is mediated by calmodulin
897 binding to Tic32. Proc. Natl. Acad. Sci. U.S.A.103, 16051-16056.
898 Courdavault, V., Papon, N., Clastre, M., Giglioli-Guivarc'h, N., St-Pierre, B., Burlat, V. (2014)
899 A look inside an alkaloid multisite plant: the *Catharanthus* logistics. Curr. Opin. Plant
900 Biol. 19, 43-50. Review
901 De Luca, V., Marineau, C., and Brisson, N. (1989). Molecular cloning and analysis of cDNA
902 encoding a plant tryptophan decarboxylase: comparison with animal dopa
903 decarboxylases. Proc. Natl. Acad. Sci. U.S.A. 86, 2582-2586.
904 De Luca, V., Salim, V., Thamm, A., Masada, S.A., and Yu, F. (2014). Making
905 iridoids/secoiridoids and monoterpenoid indole alkaloids: progress on pathway
906 elucidation. Curr. Opin. Plant Biol. 19, 35-42.
907 Fan, G., Luo, W.Z., Luo, S.H., Li, Y., Meng, X.L., Zhou, X.D., and Zhang, Y. (2014) Metabolic
908 discrimination of *Swertia mussotii* and *Swertia chirayita* known as "Zangyinchen" in
909 traditional Tibetan medicine by (1)H NMR-based metabolomics. J. Pharm. Biomed.
910 Anal. 98, 364-370.
911 Farias, F.M., Passos, C.S., Arbo, M.D., Barros, D.M., Gottfried, C., Steffen, V.M. and
912 Henriques, A.T. (2012). Strictosidinic acid, isolated from *Psychotria myriantha* Mull.

Arg. (Rubiaceae), decreases serotonin levels in rat hippocampus. Fitoterapia 83, 1138-1143.

Galili, G., Amir, R., Fernie, A.R. (2016). The Regulation of Essential Amino Acid Synthesis and Accumulation in Plants. Annu. Rev. Plant Biol. 67,153-178.

Geu-Flores, F., Sherden, N.H., Courdavault, V., Burlat, V., Glenn, W.S., Wu, C., Nims, E., Cui, Y., and O'Connor, S.E. (2012). An alternative route to cyclic terpenes by reductive cyclization in iridoid biosynthesis. Nature 492, 138-142.

Gongora-Castillo, E., Childs, K.L., Fedewa, G., Hamilton, J.P., Liscombe, D.K., Magallanes-Lundback, M., Mandadi, K.K., Nims, E., Runguphan, W., Vaillancourt, B., Varbanova-Herde, M., Dellapenna, D., McKnight, T.D., O'Connor, S., and Buell, C.R. (2012). Development of transcriptomic resources for interrogating the biosynthesis of monoterpene indole alkaloids in medicinal plant species. PloS one 7, e52506.

Gopalakrishnan, R., and Shankar, B. (2014). Multiple shoot cultures of *Ophiorrhiza rugosa* var. decumbens Deb and Mondal--a viable renewable source for the continuous production of bioactive *Camptotheca* alkaloids apart from stems of the parent plant of *Nothapodytes foetida* (Wight) Sleumer. Phytomedicine 21, 383-389.

Graikou, K., Aligiannis, N., Chinou, I.B., and Harvala, C. (2002). Cantleyoside-dimethyl-acetal and other iridoid glucosides from *Pterocephalus perennis* – antimicrobial activities. Z . Naturforsch. C 57, 95-99.

Gu, L., Jones, A.D., and Last, R.L. (2010). Broad connections in the *Arabidopsis* seed metabolic network revealed by metabolite profiling of an amino acid catabolism mutant. Plant J. 61, 579-590.

Hamzah, A.S., Arbain, D., Sargent, M.M.V. and Lajis, N.H. (1994). The Alkaloids of *Ophiorrhiza communis* and *O. tomentosa*. Pertanika J. Sci. Tech. 2, 33-38.

Han, Q.B., Li, S.L., Qiao, C.F., Song, J.Z., Cai, Z.W., Pui-Hay But, P., Shaw, P.C., and Xu, H.X. (2008) A simple method to identify the unprocessed *Strychnos* seeds used in herbal medicinal products. Planta Med. 74, 458-463.

Hellens, R., Mullineaux, P., and Klee, H. (2000). Technical Focus: a guide to *Agrobacterium* binary Ti vectors. Trends Plant Sci. 5, 446-451.

Helliwell, C.A., and Waterhouse, P.M. (2005). Constructs and methods for hairpin RNA-mediated gene silencing in plants. Methods Enzymol. 392, 24-35.

Hofer, R., Dong, L., Andre, F., Ginglinger, J.F., Lugan, R., Gavira, C., Grec, S., Lang, G., Memelink, J., Van der Krol, S., Bouwmeester, H., and Werck-Reichhart, D. (2013). Geraniol hydroxylase and hydroxygeraniol oxidase activities of the CYP76 family of cytochrome P450 enzymes and potential for engineering the early steps of the (seco)iridoid pathway. Metab. Eng. 20, 221-232.

Hutchinson, C.R., Heckendorf, A.H., Straughn, J.L., Daddona, P.E., and Cane, D.E. (1979). Biosynthesis of camptothecin. 3. Definition of strictosamide as the penultimate biosynthetic precursor assisted by carbon-13 and deuterium NMR spectroscopy. Journal of the American Chemical Society 101, 3358-3369.

Irmler, S., Schröder, G., St-Pierre, B., Crouch, N.P., Hotze, M., Schmidt, J., Strack, D., Matern, U., and Schröder, J. (2000). Indole alkaloid biosynthesis in *Catharanthus roseus*: new enzyme activities and identification of cytochrome P450 CYP72A1 as secologanin synthase. Plant J. 24, 797-804.

Itoh, A., Tanaka, Y., Nagakura, N., Akita, T., Nishi, T., and Tanahashi, T. (2008). Phenolic and iridoid glycosides from *Strychnos axillaris*. Phytochemistry 69, 1208-1214.

Kumar, K., Kumar, S.R., Dwivedi, V., Rai, A., Shukla, A.K., Shanker, K., and Nagegowda, D.A. (2015). Precursor feeding studies and molecular characterization of geraniol synthase establish the limiting role of geraniol in monoterpene indole alkaloid biosynthesis in *Catharanthus roseus* leaves. Plant Sci. 239, 56-66.

Leménager, D., Ouelhazi, L., Mahroug, S., Veau, B., St-Pierre, B., Rideau, M., Aguirreolea, J., Burlat, V., and Clastre, M. (2005). Purification, molecular cloning, and cell-specific gene expression of the alkaloid-accumulation associated protein CrPS in *Catharanthus roseus*. J. Exp. Bot. 56, 1221-1228.

Liu, Y.-Q., Li, W.-Q., Morris-Natschke, S.L., Qian, K., Yang, L., Zhu, G.-X., Wu, X.-B., Chen, A.-L., Zhang, S.-Y., Nan, X., and Lee, K.-H. (2015). Perspectives on Biologically Active Camptothecin Derivatives. Medicinal Res. Rev. 35, 753-789.

Lloyd, G. and McGown, B. (1981) Commercially-feasible micropropagation of Mountain Laurel, *Kalmia latifolia*, by shoot tip culture. Proc. Int. Plant Prop. Soc. 30, 421-427.

Lopez-Meyer, M., and Nessler, C.L. (1997). Tryptophan decarboxylase is encoded by two autonomously regulated genes in *Camptotheca acuminata* which are differentially expressed during development and stress. Plant J. 11, 1167-1175.

Lorence, A., and Nessler, C.L. (2004). Camptothecin, over four decades of surprising findings. Phytochemistry 65, 2735-2749.

Marquez, B.L. Gerwick, W.H., and Williamson R.T. (2001) Survey of NMR experiments for the determination of ^{n}J(C,H) heteronuclear coupling constants in small molecules. Magn. Reson. Chem. 39, 499-530.

Miettinen, K., Dong, L., Navrot, N., Schneider, T., Burlat, V., Pollier, J., Woittiez, L., van der Krol, S., Lugan, R., Ilc, T., Verpoorte, R., Oksman-Caldentey, K.M., Martinoia, E., Bouwmeester, H., Goossens, A., Memelink, J., and Werck-Reichhart, D. (2014). The seco-iridoid pathway from *Catharanthus roseus*. Nature Commun. 5, 3606.

Montoro, P., Maldini, M., Piacente, S., Macchia, M., and Pizza, C. (2010). Metabolite fingerprinting of *Camptotheca acuminata* and the HPLC-ESI-MS/MS analysis of camptothecin and related alkaloids. J. Pharm. Biomed. Anal. 51, 405-415.

Müller, A.A. and Weigend, M. (1998) Iridoids from *Loasa acerifolia*. Phytochem. 49,131-135

Munkert, J., Pollier, J., Miettinen, K., Van Moerkercke, A., Payne, R., Muller-Uri, F., Burlat, V., O'Connor, S.E., Memelink, J., Kreis, W., and Goossens, A. (2014). Iridoid Synthase Activity Is Common among the Plant Progesterone 5beta-Reductase Family. Mol. Plant. 8, 136-52.

Murata, J., Roepke, J., Gordon, H., and De Luca, V. (2008). The Leaf Epidermome of *Catharanthus roseus* Reveals Its Biochemical Specialization. Plant Cell 20, 524-542.

Patthy-Lukáts, Á., Károlyházy, L., Szabó, L.F., and Podányi, B. (1997). First direct and detailed stereochemical analysis of strictosidine. J. Nat. Prod. 60, 69-75.

Rastrelli, L., Caceres, A., Morales, C., De Simone, F., and Aquino, R. (1998) Iridoids from *Lippia graveolens*. Phytochem. 49, 1829-1832.

Reanmongkol, W., Subhadhirasakul, S., Kongsang, J., Tanchong, M., and Kitti, J. (2000) Analgesic and Antipyretic Activities of n-Butanol Alkaloids Extracted from the Stem Bark *Hunteria zeylanica* and its Major Constituent, Strictosidinic Acid, in Mice. Pharm. Biol. 38, 68-73.

1002 Saeed, A.I., Bhagabati, N.K., Braisted, J.C., Liang, W., Sharov, V., Howe, E.A., Li, J.,
1003 Thiagarajan, M., White, J.A., and Quackenbush, J. (2006). [9] TM4 Microarray Software
1004 Suite. Methods Enzymol. 411, 134-193.
1005 Salim, V., Yu, F., Altarejos, J., and De Luca, V. (2013). Virus-induced gene silencing identifies
1006 *Catharanthus roseus* 7-deoxyloganic acid-7-hydroxylase, a step in iridoid and
1007 monoterpene indole alkaloid biosynthesis. Plant J. 76, 754-765.
1008 Salim, V., Wiens, B., Masada-Atsumi, S., Yu, F., and De Luca, V. (2014). 7-Deoxyloganetic
1009 acid synthase catalyzes a key 3 step oxidation to form 7-deoxyloganetic acid in
1010 *Catharanthus roseus* iridoid biosynthesis. Phytochemistry 101, 23-31.
1011 Serrilli, A.M., Ramunno, A., Amicucci, F., Chicarella, V., Santoni, S., Ballero, M., Serafini, M.,
1012 and Bianco, A. (2008) Iridoidic pattern in endemic Sardinian plants: the case of *Galium*
1013 species. Nat. Prod. Res. 22, 618-622.
1014 Sheriha, G.M., and Rapoport, H. (1976). Biosynthesis of *Camptotheca acuminata* alkaloids.
1015 Phytochemistry 15, 505-508.
1016 Skaltsounis, A.L., Tillequin, F., Koch, M., Pusset, J. and Chauvière, G. (1989) Iridoids from
1017 *Scaevola racemigera.* Planta Med. 55, 191-192.
1018 Tamura, K., Peterson, D., Peterson, N., Stecher, G., Nei, M., and Kumar, S. (2011) MEGA5:
1019 Molecular Evolutionary Genetics Analysis Using Maximum Likelihood, Evolutionary
1020 Distance, and Maximum Parsimony Methods. Mol. Biol. Evol. 28, 2731-2739.
1021 Van Moerkercke, A., Steensma, P., Schweizer, F., Pollier, J., Gariboldi, I., Payne, R., Vanden
1022 Bossche, R., Miettinen, K., Espoz, J., Purnama, P.C., Kellner, F., Seppänen-Laakso, T.,
1023 O'Connor, S.E., Rischer, H., Memelink, J., and Goossens, A. (2015). The bHLH
1024 transcription factor BIS1 controls the iridoid branch of the monoterpenoid indole alkaloid
1025 pathway in *Catharanthus roseus*. Proc. Natl. Acad. Sci. U. S. A. 112, 8130-8135.
1026 Wall, M.E., Wani, M.C., Cook, C.E., Palmer, K.H., McPhail, A.T., and Sim, G.A. (1966). Plant
1027 Antitumor Agents. I. The Isolation and Structure of Camptothecin, a Novel Alkaloidal
1028 Leukemia and Tumor Inhibitor from *Camptotheca acuminata*. J. Am. Chem. Soc. 88,
1029 3888-3890.
1030 Wink, M. (2003). Evolution of secondary metabolites from an ecological and molecular
1031 phylogenetic perspective. Phytochemistry 64, 3-19.

1032 Wright, C.M., van der Merwe, M., DeBrot, A.H., and Bjornsti, M.-A. (2015). DNA
1033 Topoisomerase I Domain Interactions Impact Enzyme Activity and Sensitivity to
1034 Camptothecin. J. Biol. Chem. 290, 12068-12078.
1035 Yamazaki, M., Mochida, K., Asano, T., Nakabayashi, R., Chiba, M., Udomson, N., Yamazaki,
1036 Y., Goodenowe, D.B., Sankawa, U., Yoshida, T., Toyoda, A., Totoki, Y., Sakaki, Y.,
1037 Góngora-Castillo, E., Buell, C.R., Sakurai, T., and Saito, K. (2013). Coupling Deep
1038 Transcriptome Analysis with Untargeted Metabolic Profiling in Ophiorrhiza pumila to
1039 Further the Understanding of the Biosynthesis of the Anti-Cancer Alkaloid Camptothecin
1040 and Anthraquinones. Plant Cell Physiol. 54, 686-696.
1041 Yamazaki, Y., Sudo, H., Yamazaki, M., Aimi, N., and Saito, K. (2003a). Camptothecin
1042 Biosynthetic Genes in Hairy Roots of *Ophiorrhiza pumila*: Cloning, Characterization and
1043 Differential Expression in Tissues and by Stress Compounds. Plant Cell Physiol. 44, 395-
1044 403.
1045 Yamazaki, Y., Urano, A., Sudo, H., Kitajima, M., Takayama, H., Yamazaki, M., Aimi, N., and
1046 Saito, K. (2003b). Metabolite profiling of alkaloids and strictosidine synthase activity in
1047 camptothecin producing plants. Phytochemistry 62, 461-470.
1048 Zhang, T., Li, J., Li, B., Chen, L., Yin, H.L., Liu, S.J., Tian, Y., and Dong, J.X. (2012) Two
1049 novel secoiridoid glucosides from *Tripterospermum chinense*. J. Asian Nat. Prod. Res.
1050 14, 1097-102.
1051 Zhou, Z., Yin, W., Zhang, H., Feng, Z., and Xia, J. (2013) A new iridoid glycoside and potential
1052 MRB inhibitory activity of isolated compounds from the rhizomes of *Cyperus rotundus*
1053 L. Nat. Prod Res. 27, 1732-1736.
1054 Ziegler, J., Facchini, P.J. (2008) Alkaloid biosynthesis: metabolism and trafficking. Annu. Rev.
1055 Plant Biol. 59, 735-769. Review

TABLES

Table 1. Relevant compounds detected in wild-type *C. acuminata*. Metabolites in root, stem, shoot apex and leaf extracts were separated by a 52-minute UHPLC/MSMS method and are listed with their precursor and fragment ions. Fragment ions obtained after loss of a glucose unit (162 Da) are highlighted in bold. Only stem tissue contained detectable levels of all metabolite isomers listed here. *Note that loganic acid and secologanic acid exist also as multiple isomers that were not resolved with this UHPLC/MS method but were resolved using a different chromatography system (see Supplemental Figures S1 and S2). The last column in the table summarizes the results of *in vivo* labeling experiments with [α,α,β,β-d_4]-tryptamine in *TDC1*-RNAi plants, which do not accumulate tryptamine-derived MIAs without tryptamine supplementation. After incubation of *TDC1*-RNAi apical cuttings with [α,α,β,β-d_4]-tryptamine for six weeks, several deuterated MIAs were detectable in stem extracts. The number of deuterium atoms incorporated into detectable metabolites is indicated in the last column, with n.d. indicating compounds that were below the limit of detection in deuterium labeling experiments.

Annotated metabolite	Formula	Retention time (min)	Calculated *m/z* for $[M+H]^+$	Experimental precursor *m/z* for $[M+H]^+$	Fragment ion(s) observed in MS/MS spectra (*m/z*)	*TDC1*-RNAi Number of deuterium atoms
tryptamine (**4**)	$C_{10}H_{12}N_2$	8.0	161.1079	161.1065	144	4
loganic acid (**2**)	$C_{16}H_{24}O_{10}$	13.6 (2 isomers)*	377.1448	377.1450	359, **215**, 197, 179, 161, 151, 137, 133, 123, 109, 81	0
secologanic acid (**4**)	$C_{16}H_{22}O_{10}$	15.1 (2 isomers)*	375.1291	375.1290	**213**, 195, 177, 151, 125, 109, 107, 95, 79, 77	0

strictosidinic acid (**5**)	$C_{26}H_{32}N_2O_9$	23.9 (isomer 1) 24.8 (isomer 2) 26.5 (isomer 3)	517.2186	517.2198	500, **355**, 338, 320, 269/268, 251, 194, 180/181, 168/170, 151, 156, 144, 130, 125	n.d. (isomer 1) 4 (isomer 2) 4 (isomer 3)
strictosamide (**6**)	$C_{26}H_{30}N_2O_8$	37.6 (isomer 1) 41.5 (isomer 2)	499.2080	499.2081	**337**, 319, 267, 171, 144	4 (isomer 1) 4 (isomer 2)
strictosamide epoxide (**7**)	$C_{26}H_{30}N_2O_9$	22.8 (isomer 1) 24.8 (isomer 2) 26.5 (isomer 3)	515.2030	515.2021	**353**, 335, 309, 291, 283, 265, 263, 237, 209, 183, 184, 155, 144	n.d. (isomer 1) n.d. (isomer 2) n.d. (isomer 3)
strictosamide diol (**8**)	$C_{26}H_{32}N_2O_{10}$	20.1	533.2135	533.2170	**371**, 353, 283, 265, 185, 160, 142, 132	n.d.
strictosamide ketolactam (**9**)	$C_{26}H_{30}N_2O_{10}$	22.5 (isomer 1) 22.7 (isomer 2)	531.1979	531.1953	**369**, 351, 341, 299, 281, 271, 253, 194, 176, 158, 148, 130, 124, 106	n.d. (isomer 1) n.d. (isomer 2)
pumiloside (**10**)	$C_{26}H_{28}N_2O_9$	30.2 (isomer 1) 32.9 (isomer 2)	513.1873	513.1890	**351**, 333, 315, 305, 281, 235, 140	2 (isomer 1) n.d. (isomer 2)
deoxypumiloside (**11**)	$C_{26}H_{28}N_2O_8$	36.1 (isomer 1) 38.2 (isomer 2)	497.1924	497.1930	**335**, 265, 247, 219, 183, 169, 142, 97	2 (isomer 1) 2 (isomer 2)
camptothecin (**12**)	$C_{20}H_{16}N_2O_4$	34.3	349.1188	349.1198	305, 277, 249, 219/220, 168	2

Table 2. NMR chemical shifts and coupling constants for strictosidinic acid isomers isolated from *C. acuminata* leaf tissue as measured from J-resolved ^{1}H spectra and ^{1}H-^{13}C cHSQC spectra. Notable differences in ^{1}H chemical shifts and $^{1}J_{C\text{-}H}$ coupling constants were observed for position 21 (highlighted in bold in the table).

Carbon number and group	Isomer 2		Isomer 3	
	^{1}H shift (ppm) and $^{3}J_{H\text{-}H}$ coupling constants (Hz)	^{13}C shift (ppm) and $^{1}J_{C\text{-}H}$ coupling constants (Hz)	^{1}H shift (ppm) and $^{3}J_{H\text{-}H}$ coupling constants (Hz)	^{13}C shift (ppm) and $^{1}J_{C\text{-}H}$ coupling constants (Hz)
3 (CH)	4.45 (dd), ^{3}J = 3.4, 7.7 Hz	50.8, ^{1}J = 144 Hz	4.56 (dd), ^{3}J = 3.6, 7.9 Hz	53.1, ^{1}J = 143 Hz
5 (CH_2)	3.29 (m) 3.75 (m)	41.3, ^{1}J = 143, 145 Hz;	3.45 (m) 3.50 (m)	39.6, ^{1}J = 139, 141 Hz
6 (CH_2)	3.01 (m) 3.29 (m)	18.1, ^{1}J = 131, 133 Hz	2.99 (m) 3.04 (m)	18.2, ^{1}J = 129, 131 Hz
9 (CH)	7.56 (d), ^{3}J = 7.9 Hz	117.7, ^{1}J = 159 Hz	7.55 (d), ^{3}J = 7.9 Hz	117.6, ^{1}J = 158 Hz
10 (CH)	7.15, ^{3}J = 7.4 Hz	119.1, ^{1}J = 159 Hz	7.13, ^{3}J = 7.3 Hz	118.9, ^{1}J = 158 Hz
11 (CH)	7.23, ^{3}J = 7.6 Hz	121.9, ^{1}J = 159 Hz	7.23, ^{3}J = 7.6 Hz	121.8, ^{1}J = 158 Hz
12 (CH)	7.42, ^{3}J = 8.2 Hz	110.7, ^{1}J = 159 Hz	7.45, ^{3}J = 8.2 Hz	110.8, ^{1}J = 158 Hz
14 (CH_2)	2.15 (dd), ^{3}J = 4.6, 11.1 Hz; 2.40 (dd), ^{3}J = 5.9, 11.6 Hz	33.7, ^{1}J = 128, 129 Hz	1.98 (m) 2.46 (m)	34.1, ^{1}J = 130, 131 Hz
15 (CH)	3.00 (m)	32.6, ^{1}J = 137 Hz	2.96 (m)	32.9, ^{1}J = 135 Hz
17 (CH)	7.67 (s)	151.7, ^{1}J = 191 Hz	7.35 (s)	148.4, ^{1}J = 192 Hz
18 (CH_2)	5.32 (d), ^{3}J = 10.7 Hz; 5.43 (d), ^{3}J = 17.3 Hz	117.5, ^{1}J = 155, 158 Hz	5.39 (d), ^{3}J = 11.0 Hz; 5.47 (d), ^{3}J = 17.3 Hz	118.4, ^{1}J = 154, 161 Hz
19 (CH)	5.96 (dd), ^{3}J = 10.3, 17.5 Hz	134.8, ^{1}J = 156 Hz	6.19 (dd), ^{3}J = 10.2, 17.2 Hz	134.8, ^{1}J = 152 Hz
20 (CH)	2.70 (m)	44.2, ^{1}J = 134 Hz	2.74 (m)	44.9, ^{1}J = 132 Hz
21 (CH)	**5.93 (d), ^{3}J = 9.5 Hz**	**95.1, ^{1}J = 170 Hz**	**5.64 (d), ^{3}J = 8.2 Hz**	**95.5, ^{1}J = 178 Hz**
1′ (CH)	4.92 (d), ^{3}J = 8.0 Hz	98.9, ^{1}J = 163 Hz	4.85 (d), ^{3}J = 7.9 Hz	98.8, ^{1}J = 162 Hz
2′ (CH)	3.44 (m)	76.5, ^{1}J = 145 Hz	3.41 (m)	76.5, ^{1}J = 145 Hz

3′ (CH)	3.41 (m)	77.3, ^{1}J = 145 Hz	3.35 (m)	77.3, ^{1}J = 145 Hz
4′ (CH)	3.26 (m)	70.2, ^{1}J = 145 Hz	3.28 (m)	70.3, ^{1}J = 145 Hz
5′ (CH)	3.24 (m)	73.3, ^{1}J = 145 Hz	3.24 (m)	73.3, ^{1}J = 145 Hz
6′ (CH_2)	3.68 (dd), ^{3}J = 4.95, 12.2 Hz; 4.12 (dd), ^{3}J = 2.17, 12.1 Hz	61.6, ^{1}J = 141, 142 Hz	3.76 (dd), ^{3}J = 6.61, 12.3 Hz; 4.05 (dd), ^{3}J = 2.40, 12.6 Hz	61.5, ^{1}J = 131, 132 Hz

Table 3. Isomer compositions of strictosidinic acid and post-strictosidinic acid metabolites in different tissues of *CYC1*-RNAi lines compared to wild type. Tissues were collected from plants grown under greenhouse cultivation for eight months and metabolite levels determined by UHPLC/MS. Average levels expressed as response per kg fresh weight are shown with SD for biological replicates. For wild type, three plants independently derived from tissue culture were analyzed and for *CYC1*-RNAi lines, five plants from independently derived transgenic events were analyzed. Asterisks indicate significantly different metabolite levels in *CYC1*-RNAi lines (unpaired t-test; *, P<0.05; **, P<0.001) relative to wild type. n.d., below the limit of quantification, which is defined as signal/noise = 10.

Metabolite	Isomer	Wild type					*CYC1*-RNAi				
		Root	Stem	Shoot Apex	Young Leaf	Mature Leaf	Root	Stem	Shoot Apex	Young Leaf	Mature Leaf
Strictosidinic acid	1	n.d.	447±147	475±87	342±54	n.d.	n.d.	n.d.**	130±116**	42±58**	n.d.
	2	997±298	3970±1098	45252±3958	40524±3540	2808±1220	155±112**	1025±822*	3436±1811**	2742±884**	2070±733
	3	23477±5219	30066±5284	62147±4213	50004±2840	4400±1379	3020±1826**	1209±712**	8022±4086**	2381±1108**	49±67**

Strictosamide	**1**	936±175	1511±264	249±41	n.d.	n.d.	n.d.**	n.d.**	n.d.**	n.d.	n.d.
	2	323±65	222±24	975±121	1305±107	1306±170	165±74*	21±13**	125±35**	132±35**	149±127**
Pumiloside	**1**	219±90	520±130	n.d.	n.d.	n.d.	n.d.**	152±90*	n.d.	n.d.	n.d.
	2	28±11	360±25	1329±167	928±153	179±65	n.d.**	n.d.**	127±45**	n.d.**	n.d.**
Deoxypumiloside	**1**	373±66	1291±141	n.d.	n.d.	n.d.	63±61**	372±169**	n.d.	n.d.	n.d.
	2	955±203	1266±395	111±88	n.d.	n.d.	165±85**	436±108*	n.d.	n.d.	n.d.

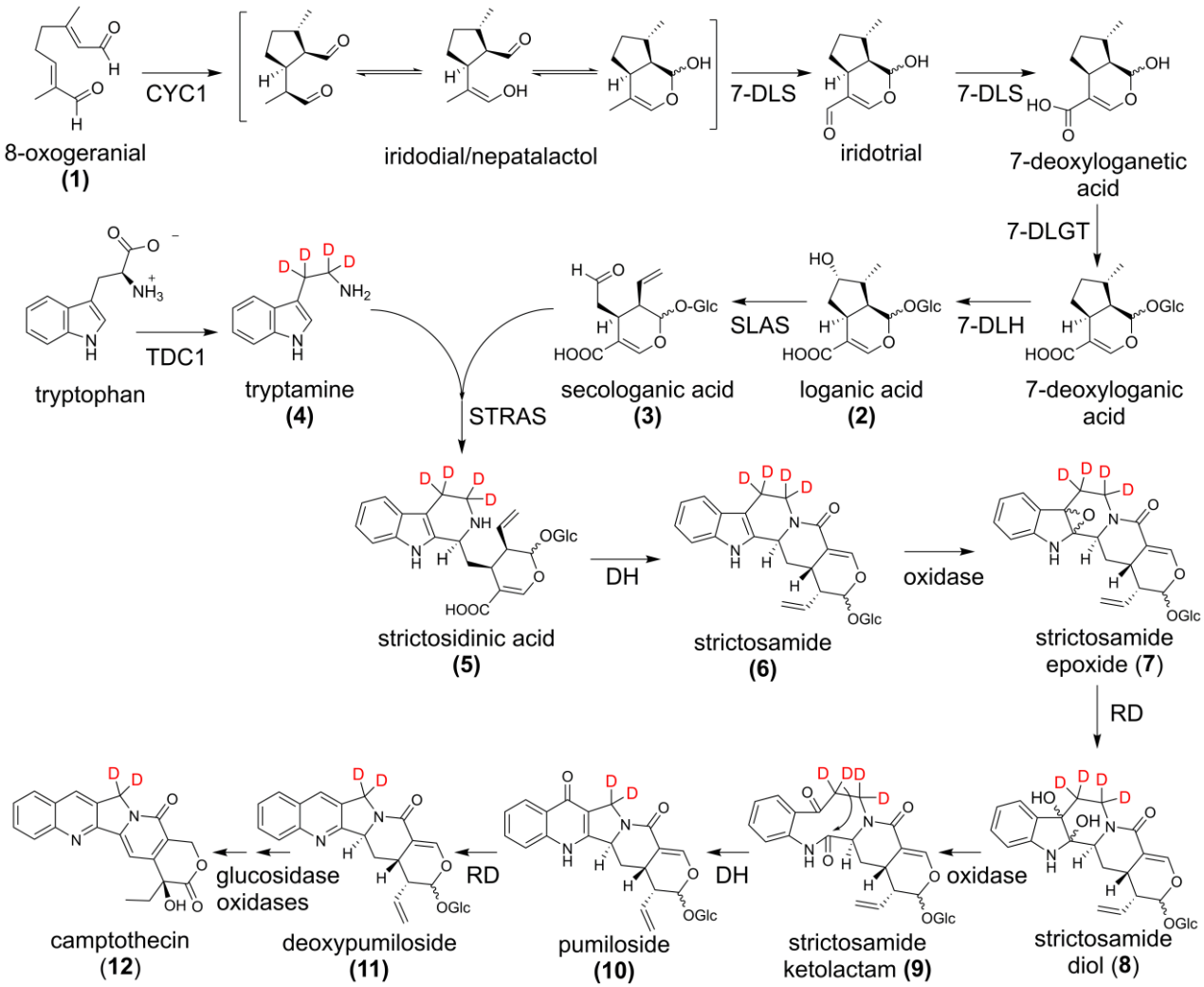

Figure 1. Proposed pathway for camptothecin biosynthesis in *C. acuminata*. Camptothecin (**12**) is synthesized from the central precursor strictosidinic acid (**5**) derived from condensation of tryptamine (**4**) and the iridoid secologanic acid (**3**), a monoterpenoid glycoside. *In vivo* labeling experiments with deuterated [α,α,β,β-d_4]-tryptamine resulted in labeling of strictosidinic acid and downstream metabolites with the number and the likely positions of deuterium (D) indicated in red. Enzyme activities are indicated. TDC1 and CYC1 were identified and characterized in the present study. 7-DLS, 7-deoxyloganetic acid synthase; 7-DLGT, 7-deoxyloganetic acid glucosyltransferase; 7-DLH, 7-deoxyloganic acid hydroxylase; SLAS, secologanic acid synthase; STRAS, strictosidinic acid synthase; DH, dehydration: RD, reduction.

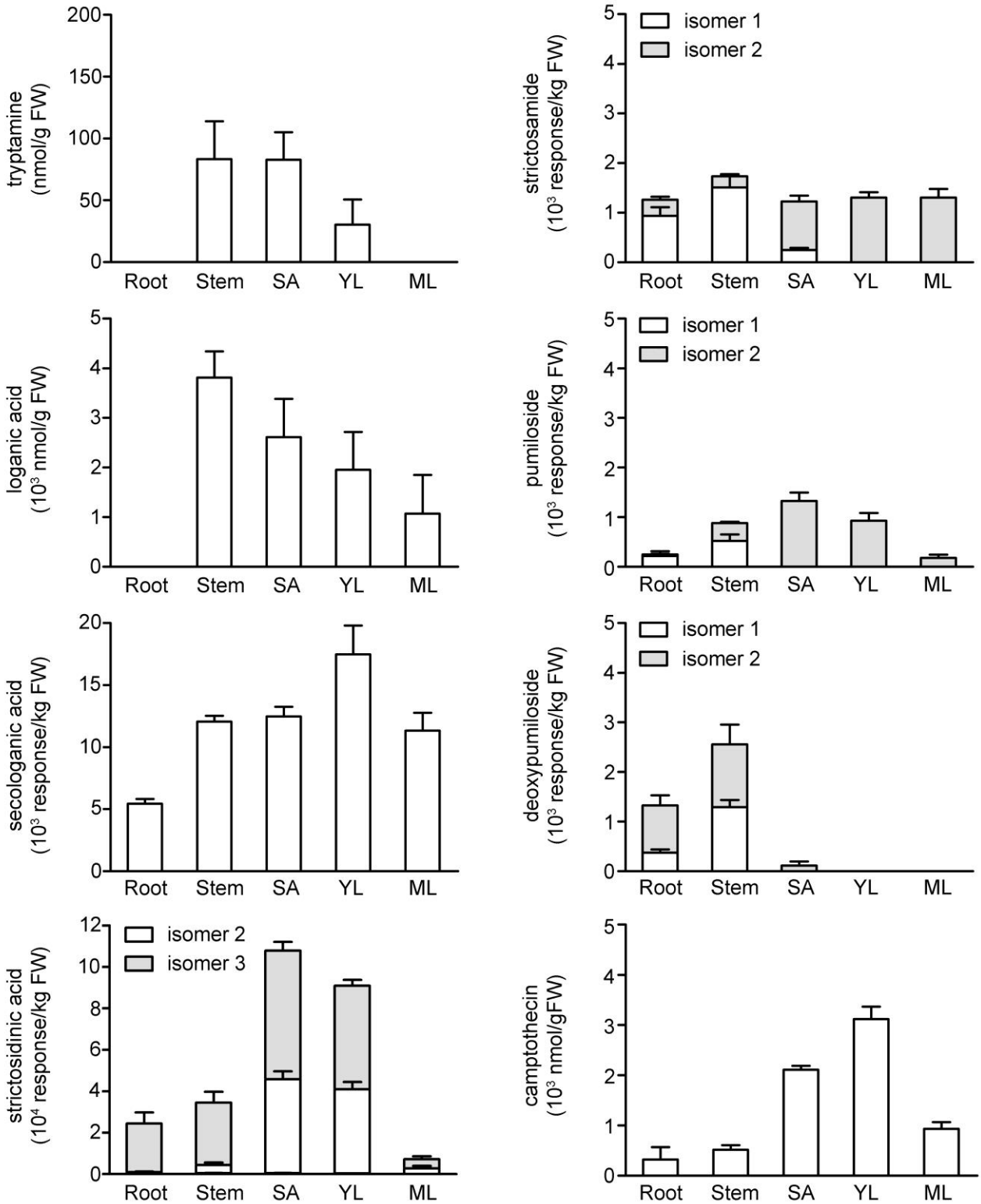

Figure 2. Tissue distribution profiles of proposed camptothecin pathway metabolites in wild-type *C. acuminata*. Tissues were collected from wild-type plants that had been under greenhouse cultivation in soil for eight months and 70% acetonitrile extracts were analyzed using a 15-min gradient elution method for UHPLC/MS. Multiple isomers were detected for strictosidinic acid (Figure 1, compound **5**) and post-strictosidinic acid metabolites (Figure 1, compounds **6**, **10, 11, 12**). Average values are shown with SD (n = 3) for the most abundant and quantifiable isomers (SA, shoot apex; YL: young leaf; ML: mature leaf).

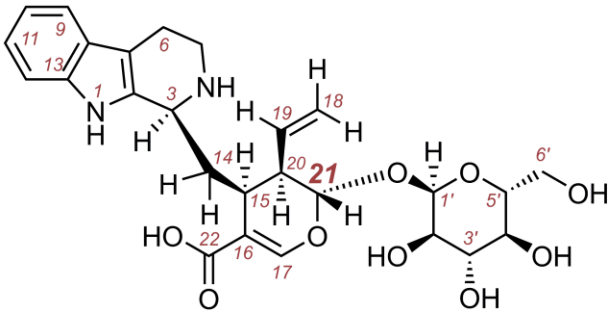

21*S* (isomer 2)

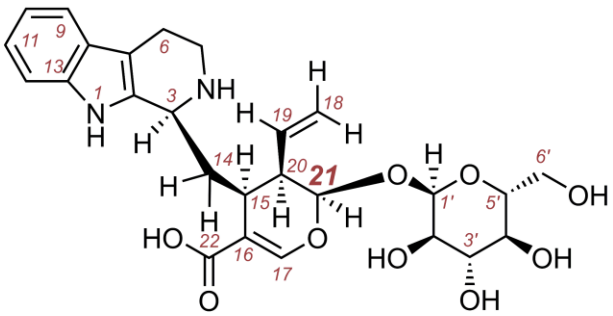

21*R* (isomer 3)

Figure 3. Structures of the two major strictosidinic acid isomers isolated from *C. acuminata* leaf tissue. NMR analyses (Table 2) show that the two major strictosidinic acid isomers (isomers 2 and 3) differ in stereochemical configuration at position C21, the site of glucosylation.

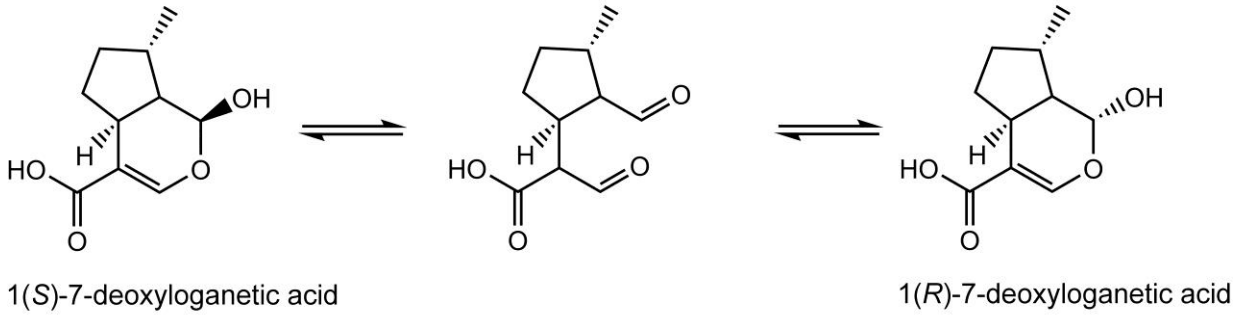

Figure 4. Formation of iridoid diastereomers. Equilibrium between the open and closed ring conformations of 7-deoxyloganetic acid yields diastereomers at the C2 hydroxyl group.

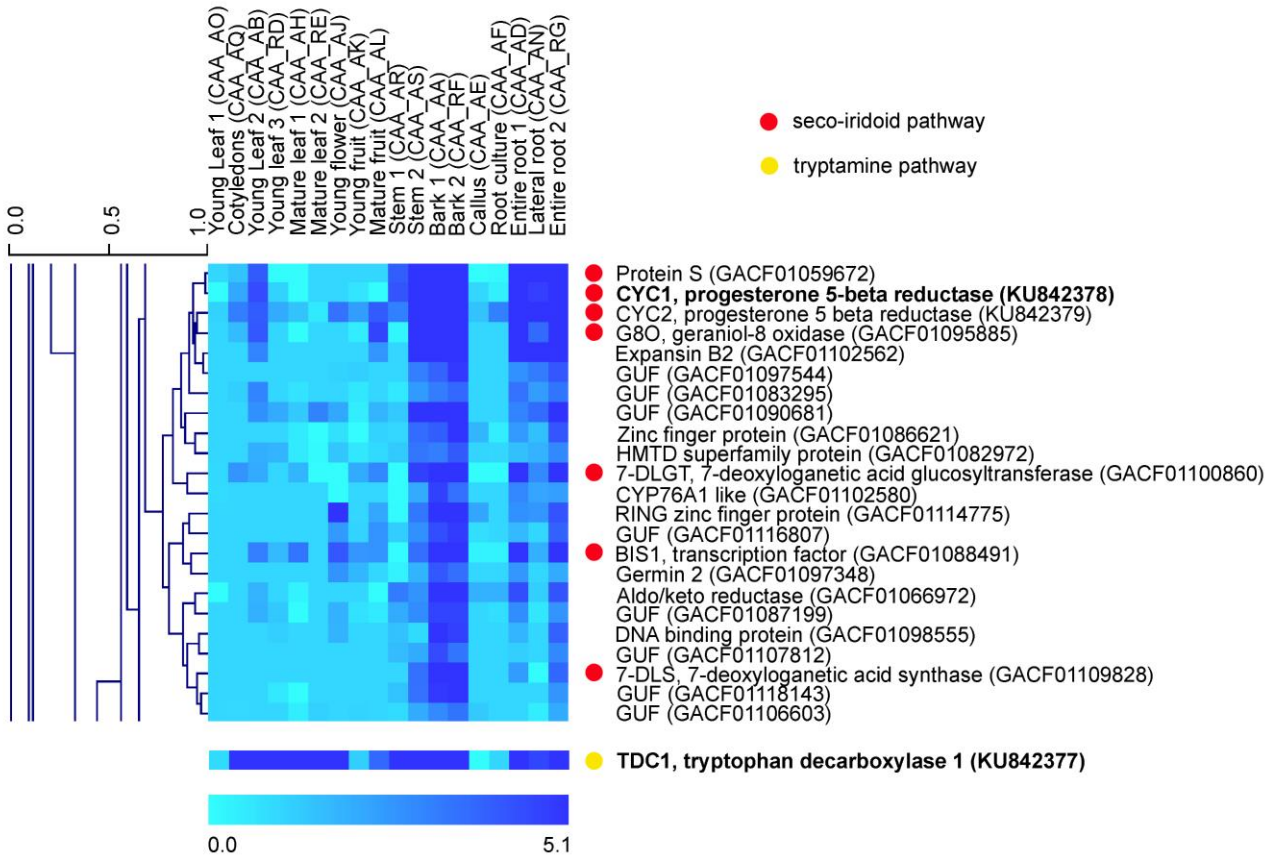

Figure 5. Heat map of expression data of candidate genes for the seco-iridoid branch of camptothecin biosynthesis. Hierarchical clustering of 25,725 transcripts was generated based on average linkage of Pearson correlation coefficients of $\log_2$-transformed FPKM (fragments per kb transcript per million mapped reads) expression values from the MPGR website (http://medicinalplantgenomics.msu.edu/) with Multi-experiment Viewer software package MeV v4.9 (Saeed et al., 2006). A subcluster encompassing 23 genes is shown with GenBank accession numbers listed in parentheses. The color scale depicts transcript abundance (expressed as $\log_2$-transformed FPKM). Red dots indicate the position of candidates for the seco-iridoid pathway and for comparison, the expression profile (expressed as $\log_2$-transformed FPKM) of *TDC1* is shown (yellow dot). *CYC1* and *TDC1*, both highlighted in bold, have been characterized in this study. Note that lists of candidate genes, GenBank accession numbers, Medicinal Plant Genome Resource transcript identifiers and FPKM values are given in Supplemental Data Sets 2 and 3. Abbreviations used: HMTD, heavy metal transport/detoxification; GUF, gene of unknown function.

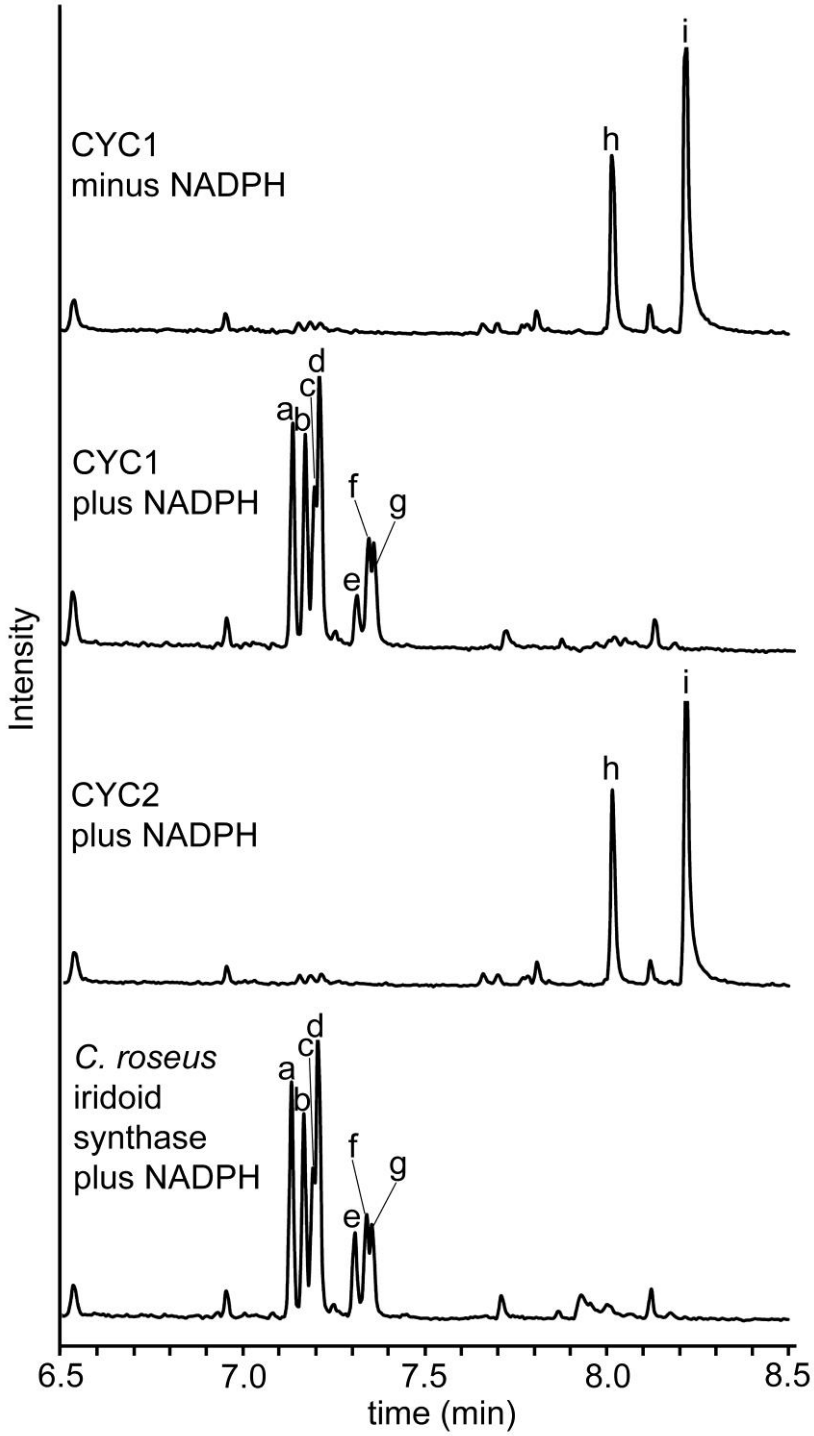

Figure 6. Iridoid synthase assay with recombinant CYC1 and CYC2 enzymes. Purified recombinant proteins were assayed for iridoid synthase activity in reaction mixtures with 8-oxogeranial (Figure 1, compound **1**) in the absence or presence of NADPH. Assays were extracted with dichloromethane and analyzed by GC/MS. The respective total ion chromatograms are shown in comparison to that obtained for a control assay with *C. roseus* iridoid synthase (**a** – **g**, reaction products; **h** and **i**, 8-oxoneral and 8-oxogeranial substrates, respectively). In the presence of NADPH, CYC1 and *C. roseus* iridoid synthase catalyzed conversion of the substrate to reduction products while no products were detectable in assays with CYC2. Incubation of the proteins in reaction mixtures lacking NADPH did not result in detectable products; CYC1 minus NADPH is shown as a representative trace.

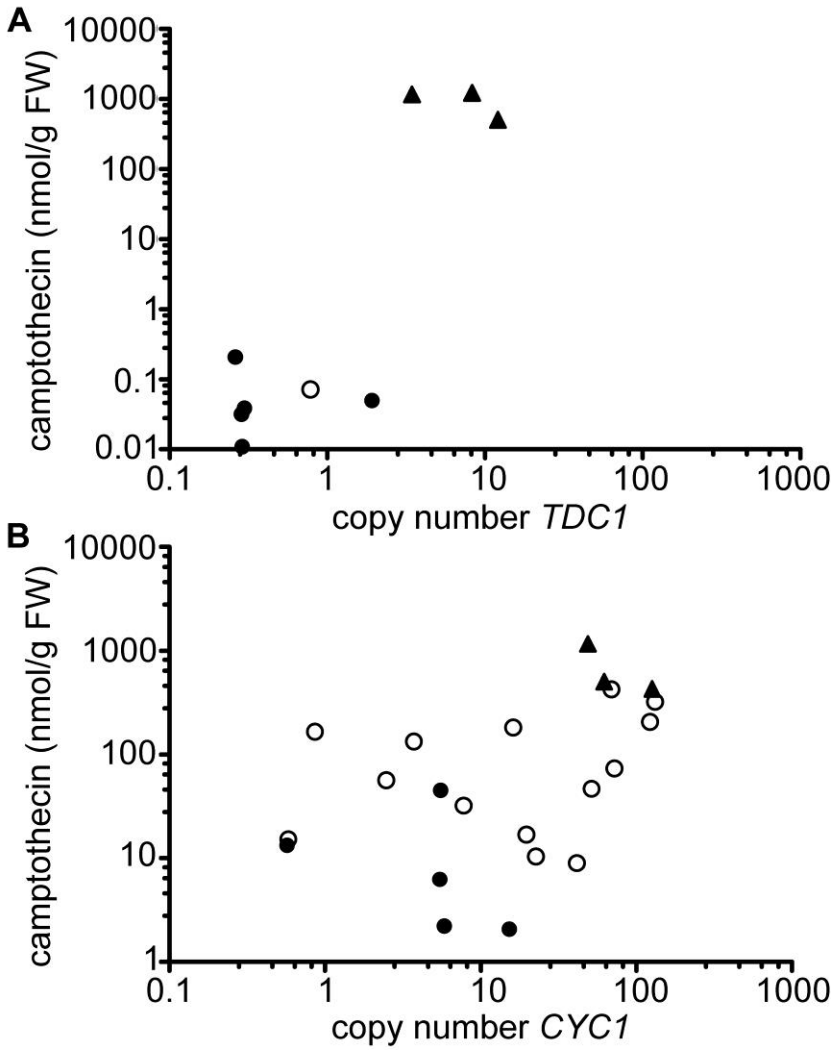

Figure 7. Correlation analyses between stem transcript abundance of the RNAi-targeted gene with the mature leaf camptothecin content of transgenic RNAi plants (open and filled circles) and wild-type plants (filled triangles). Data are shown for *TDC1*-RNAi plants **(A)** and for *CYC1*-RNAi plants **(B)** in comparison to wild type plants. Each circle represents one RNAi plant from an independent transformation event, with filled circles indicating lines that were selected for further in-depth analyses. For wild type, three independent lines were taken through tissue culture and regeneration. Stems and mature leaves were collected from plants that had been under greenhouse cultivation in soil for approximately four months. Note that the values are plotted on double $\log_{10}$ scale.

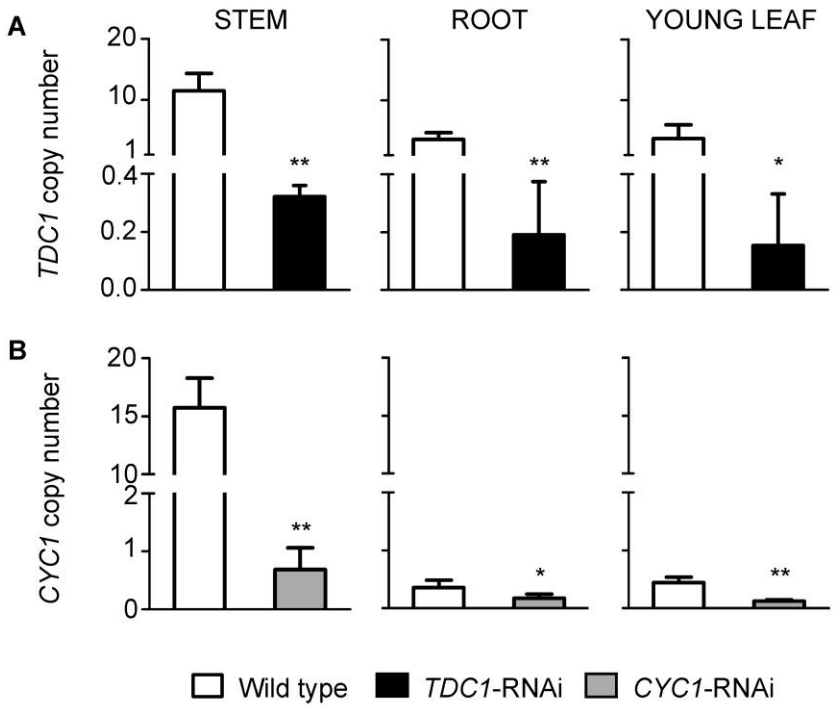

Figure 8. Expression analyses of the RNAi-targeted gene in root, young stems and young leaves of *TDC1*-RNAi plants and *CYC1*-RNAi plants relative to wild type. Tissues were collected from plants that had been under greenhouse cultivation for eight months. Average transcript copy numbers were normalized to *ACTIN6* mRNA (n = 5 and 3 for RNAi and wild type plants, respectively) and are shown for *TDC1*-RNAi plants (**A**) and *CYC1*-RNAi plants (**B**) relative to wild type. Note that the y-axis is discontinuous to allow depiction of the significant differences in RNAi-target gene copy numbers between wild type and RNAi lines. Asterisks indicate significant differences in RNAi plants (unpaired t-test; *, $P<0.05$; **, $P<0.001$) relative to wild type.

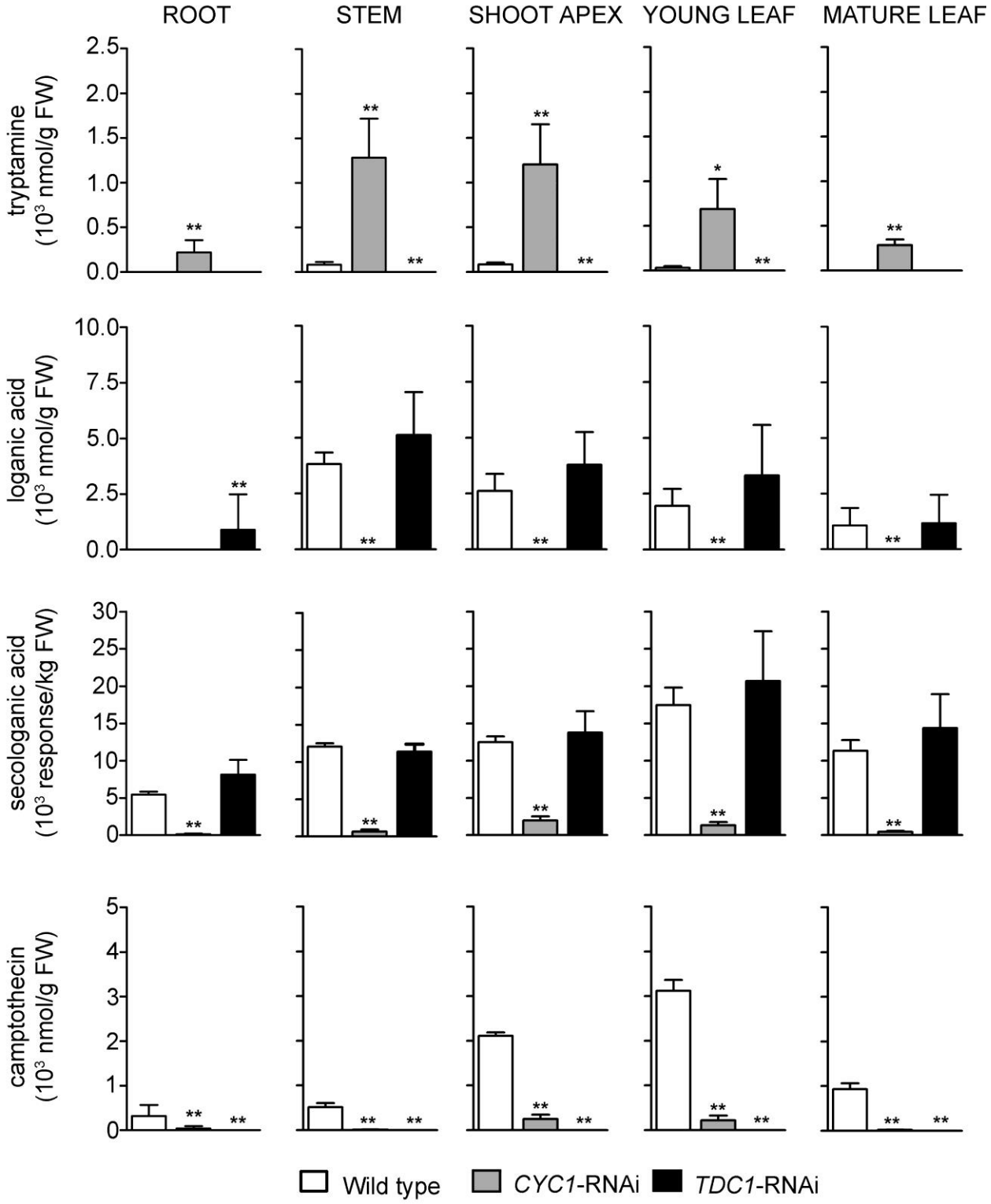

Figure 9. Levels of tryptamine, loganic acid, secologanic acid and camptothecin in different tissues of wild-type *C. acuminata* and *CYC1*-RNAi and *TDC1*-RNAi plants. Tissues were collected from plants that had been under greenhouse cultivation for eight months. Average levels of tryptamine, loganic acid, secologanic acid and camptothecin (Figure 1, compounds **4**, **2**, **3** and **12** respectively) are shown with SD for wild type (WT, n = 3), *CYC1*-RNAi (n = 5) and *TDC1*-RNAi lines (n = 5). Asterisks indicate significantly different metabolite levels in *CYC1*-RNAi lines and *TDC1*-RNAi (unpaired t-test; *, P<0.05; **, P<0.001) relative to wild type.

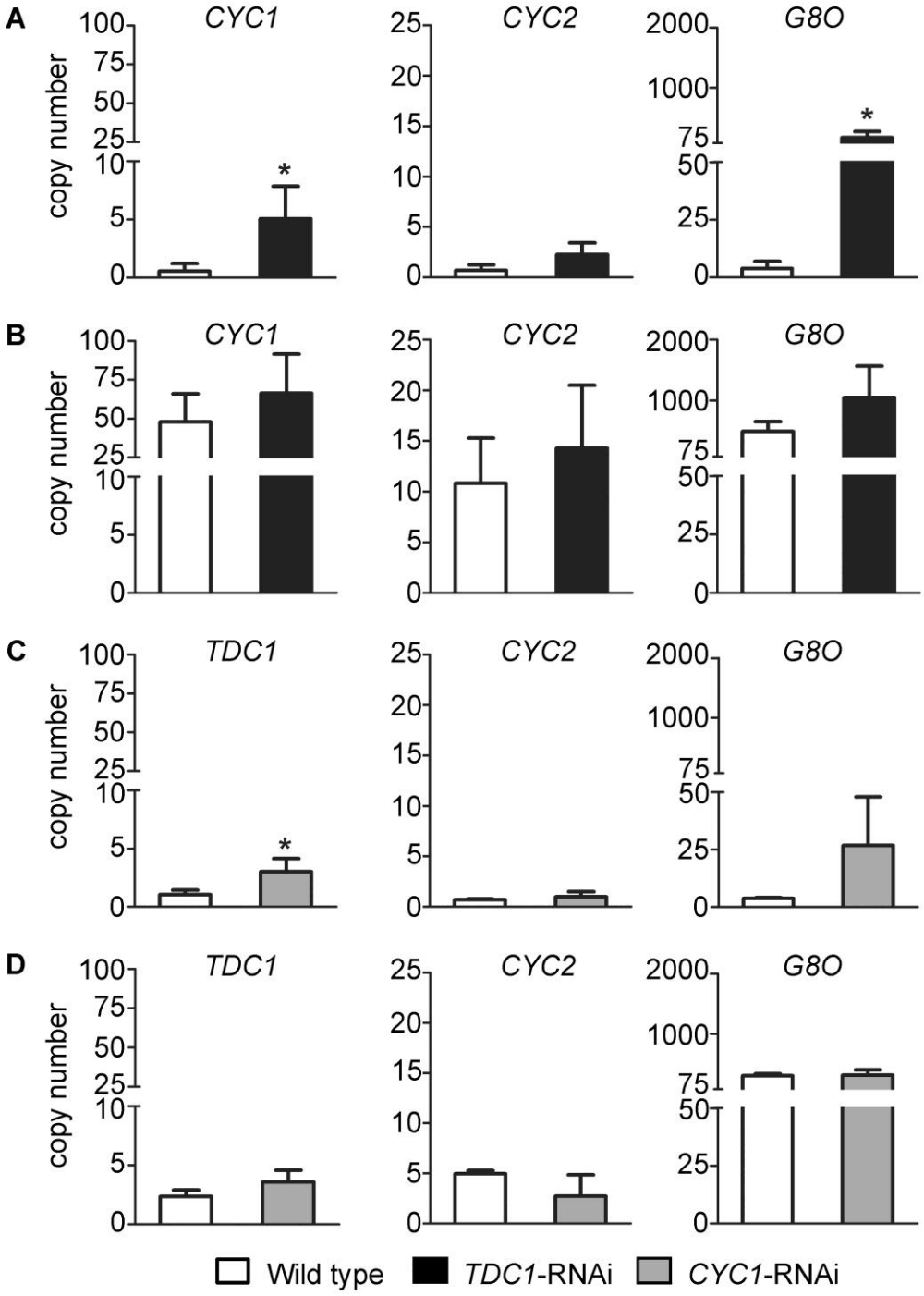

Figure 10. Root and stem expression of pathway genes not targeted by RNAi in *TDC1*-RNAi and *CYC1*-RNAi plants in comparison to wild type. Tissues were collected from RNAi plants that had been under greenhouse cultivation for eight months. mRNA levels for *CYC1*, *CYC2* and *G8O* in roots (A) and stems (B) of *TDC1*-RNAi and wild type (WT) plants are shown. (C) and (D) are root and stem transcript levels, respectively, for *TDC1*, *CYC2,* and *G8O* in *CYC1*-RNAi plants compared to wild type (WT). Average transcript copy numbers were normalized to *ACTIN6* mRNA for RNAi and wild type plants (n = 5 and 3, respectively). Asterisks indicate significant differences in RNAi plants in comparison to wild type (unpaired t-test; *, P<0.05). Note that the Y-axis scales for *CYC2* and *G8O* are different from *CYC1* and *TDC1*.

Parsed Citations

Aberham, A., Pieri, V., Croom, E.M. Jr, Ellmerer, E., and Stuppner, H. (2011) Analysis of iridoids, secoiridoids and xanthones in Centaurium erythraea, Frasera caroliniensis and Gentiana lutea using LC-MS and RP-HPLC. J. Pharm. Biomed. Anal. 54, 517-525.
Pubmed: Author and Title
CrossRef: Author and Title
Google Scholar: Author Only Title Only Author and Title

Aimi, N., Nishimura, M., Miwa, A., Hoshino, H., Sakai, S., and Haginiwa, J. (1989). Pumiloside and deoxypumiloside; plausible intermediate of camptothecin biosynthesis. Tetrahedron Lett. 30, 4991-4994.
Pubmed: Author and Title
CrossRef: Author and Title
Google Scholar: Author Only Title Only Author and Title

Ajala, O.S., Piggott, A.M., Plisson, F., Khalil, Z., Huang, X., Adesegun, S.A., Coker, H.A.B. and Capon, R.J. (2011) Ikirydinium A: a new indole alkaloid from the seeds of Hunteria umbellata (K. Schum). Tetrahedron Lett. 52, 7125-7127.
Pubmed: Author and Title
CrossRef: Author and Title
Google Scholar: Author Only Title Only Author and Title

Arbain, D., Putra, D.P., and Sargent. M.V. (1993) The Alkaloids of Ophiorrhiza filistipula. Australian J. Chem. 46(7) 977 - 985.
Pubmed: Author and Title
CrossRef: Author and Title
Google Scholar: Author Only Title Only Author and Title

Asada, K., Salim, V., Masada-Atsumi, S., Edmunds, E., Nagatoshi, M., Terasaka, K., Mizukami, H., and De Luca, V. (2013). A 7-deoxyloganetic acid glucosyltransferase contributes a key step in secologanin biosynthesis in Madagascar periwinkle. Plant Cell 25, 4123-4134.
Pubmed: Author and Title
CrossRef: Author and Title
Google Scholar: Author Only Title Only Author and Title

Asano, T., Kobayashi, K., Kashihara, E., Sudo, H., Sasaki, R., Iijima, Y., Aoki, K., Shibata, D., Saito, K., and Yamazaki, M. (2013). Suppression of camptothecin biosynthetic genes results in metabolic modification of secondary products in hairy roots of Ophiorrhiza pumila. Phytochemistry 91, 128-139.
Pubmed: Author and Title
CrossRef: Author and Title
Google Scholar: Author Only Title Only Author and Title

Banerjee, A., and Sharkey, T.D. (2014). Methylerythritol 4-phosphate (MEP) pathway metabolic regulation. Nat. Prod Rep. 31, 1043-1055. Review.
Pubmed: Author and Title
CrossRef: Author and Title
Google Scholar: Author Only Title Only Author and Title

Bedewitz, M.A., Gongora-Castillo, E., Uebler, J.B., Gonzales-Vigil, E., Wiegert-Rininger, K.E., Childs, K.L., Hamilton, .P., Vaillancourt, B., Yeo, Y.S., Chappell, J., DellaPenna, D., Jones, A.D., Buell, C. R. and Barry, C. S. (2014) A root-expressed L-phenylalanine:4-hydroxyphenylpyruvate aminotransferase is required for tropane alkaloid biosynthesis in Atropa belladonna. Plant Cell 26, 3745-3762.
Pubmed: Author and Title
CrossRef: Author and Title
Google Scholar: Author Only Title Only Author and Title

Birtic, S., and Kranner, I. (2006). Isolation of high-quality RNA from polyphenol-, polysaccharide- and lipid-rich seeds. Phytochem. Anal. 17, 144-148.
Pubmed: Author and Title
CrossRef: Author and Title
Google Scholar: Author Only Title Only Author and Title

Bracher, D., and Kutchan, T.M. (1992). Strictosidine synthase from Rauvolfia serpentina: analysis of a gene involved in indole alkaloid biosynthesis. Arch. Biochem. Biophys. 294, 717-723.
Pubmed: Author and Title
CrossRef: Author and Title
Google Scholar: Author Only Title Only Author and Title

Cardoso, C.L., Castro-Gamboa, I., Silva, D.H., Furlan, M., Epifanio Rde, A., Pinto Ada, C., Moraes de Rezende, C., Lima, J.A., and Bolzani Vda, S. (2004) Indole glucoalkaloids from Chimarrhis turbinata and their evaluation as antioxidant agents and acetylcholinesterase inhibitors. J. Nat. Prod. 67, 1882-1885.
Pubmed: Author and Title
CrossRef: Author and Title
Google Scholar: Author Only Title Only Author and Title

Carte, B.K., DeBrosse, C., Eggleston, D., Hemling, M., Mentzer, M., Poehland, B., Troupe, N., Westley, J.W., and Hecht, S.M. (1990). Isolation and characterization of a presumed biosynthetic precursor of camptothecin from extracts of Camptotheca acuminata. Tetrahedron 46, 2747-2760.
Pubmed: Author and Title
CrossRef: Author and Title
Google Scholar: Author Only Title Only Author and Title

Chigri, F., Hörmann, F., Stamp, A., Stammers, D.K., Bölter, B., Soll, J., and Vothknecht, U.C. (2006). Calcium regulation of chloroplast protein translocation is mediated by calmodulin binding to Tic32. Proc. Natl. Acad. Sci. U.S.A.103, 16051-16056.
Pubmed: Author and Title
CrossRef: Author and Title
Google Scholar: Author Only Title Only Author and Title

Courdavault, V., Papon, N., Clastre, M., Giglioli-Guivarc'h, N., St-Pierre, B., Burlat, V. (2014) A look inside an alkaloid multisite plant: the Catharanthus logistics. Curr. Opin. Plant Biol. 19, 43-50. Review
Pubmed: Author and Title
CrossRef: Author and Title
Google Scholar: Author Only Title Only Author and Title

De Luca, V., Marineau, C., and Brisson, N. (1989). Molecular cloning and analysis of cDNA encoding a plant tryptophan decarboxylase: comparison with animal dopa decarboxylases. Proc. Natl. Acad. Sci. U.S.A. 86, 2582-2586.
Pubmed: Author and Title
CrossRef: Author and Title
Google Scholar: Author Only Title Only Author and Title

De Luca, V., Salim, V., Thamm, A., Masada, S.A., and Yu, F. (2014). Making iridoids/secoiridoids and monoterpenoid indole alkaloids: progress on pathway elucidation. Curr. Opin. Plant Biol. 19, 35-42.
Pubmed: Author and Title
CrossRef: Author and Title
Google Scholar: Author Only Title Only Author and Title

Fan, G., Luo, W.Z., Luo, S.H., Li, Y., Meng, X.L., Zhou, X.D., and Zhang, Y. (2014) Metabolic discrimination of Swertia mussotii and Swertia chirayita known as "Zangyinchen" in traditional Tibetan medicine by (1)H NMR-based metabolomics. J. Pharm. Biomed. Anal. 98, 364-370.
Pubmed: Author and Title
CrossRef: Author and Title
Google Scholar: Author Only Title Only Author and Title

Farias, F.M., Passos, C.S., Arbo, M.D., Barros, D.M., Gottfried, C., Steffen, V.M. and Henriques, A.T. (2012). Strictosidinic acid, isolated from Psychotria myriantha Mull. Arg. (Rubiaceae), decreases serotonin levels in rat hippocampus. Fitoterapia 83, 1138-1143.
Pubmed: Author and Title
CrossRef: Author and Title
Google Scholar: Author Only Title Only Author and Title

Galili, G., Amir, R., Fernie, A.R. (2016). The Regulation of Essential Amino Acid Synthesis and Accumulation in Plants. Annu. Rev. Plant Biol. 67,153-178.
Pubmed: Author and Title
CrossRef: Author and Title
Google Scholar: Author Only Title Only Author and Title

Geu-Flores, F., Sherden, N.H., Courdavault, V., Burlat, V., Glenn, W.S., Wu, C., Nims, E., Cui, Y., and O'Connor, S.E. (2012). An alternative route to cyclic terpenes by reductive cyclization in iridoid biosynthesis. Nature 492, 138-142.
Pubmed: Author and Title
CrossRef: Author and Title
Google Scholar: Author Only Title Only Author and Title

Gongora-Castillo, E., Childs, K.L., Fedewa, G., Hamilton, J.P., Liscombe, D.K., Magallanes-Lundback, M., Mandadi, K.K., Nims, E., Runguphan, W., Vaillancourt, B., Varbanova-Herde, M., Dellapenna, D., McKnight, T.D., O'Connor, S., and Buell, C.R. (2012). Development of transcriptomic resources for interrogating the biosynthesis of monoterpene indole alkaloids in medicinal plant species. PloS one 7, e52506.
Pubmed: Author and Title
CrossRef: Author and Title
Google Scholar: Author Only Title Only Author and Title

Gopalakrishnan, R., and Shankar, B. (2014). Multiple shoot cultures of Ophiorrhiza rugosa var. decumbens Deb and Mondal--a viable renewable source for the continuous production of bioactive Camptotheca alkaloids apart from stems of the parent plant of Nothapodytes foetida (Wight) Sleumer. Phytomedicine 21, 383-389.
Pubmed: Author and Title
CrossRef: Author and Title
Google Scholar: Author Only Title Only Author and Title

Graikou, K., Aligiannis, N., Chinou, I.B., and Harvala, C. (2002). Cantleyoside-dimethyl-acetal and other iridoid glucosides from Pterocephalus perennis - antimicrobial activities. Z. Naturforsch. C 57, 95-99.
Pubmed: Author and Title
CrossRef: Author and Title
Google Scholar: Author Only Title Only Author and Title

Gu, L., Jones, A.D., and Last, R.L. (2010). Broad connections in the Arabidopsis seed metabolic network revealed by metabolite profiling of an amino acid catabolism mutant. Plant J. 61, 579-590.
Pubmed: Author and Title
CrossRef: Author and Title
Google Scholar: Author Only Title Only Author and Title

Hamzah, A.S., Arbain, D., Sargent, M.M.V. and Lajis, N.H. (1994). The Alkaloids of Ophiorrhiza communis and O. tomentosa. Pertanika J. Sci. Tech. 2, 33-38.
Pubmed: Author and Title

CrossRef: Author and Title
Google Scholar: Author Only Title Only Author and Title

Han, Q.B., Li, S.L., Qiao, C.F., Song, J.Z., Cai, Z.W., Pui-Hay But, P., Shaw, P.C., and Xu, H.X. (2008) A simple method to identify the unprocessed Strychnos seeds used in herbal medicinal products. Planta Med. 74, 458-463.
Pubmed: Author and Title
CrossRef: Author and Title
Google Scholar: Author Only Title Only Author and Title

Hellens, R., Mullineaux, P., and Klee, H. (2000). Technical Focus: a guide to Agrobacterium binary Ti vectors. Trends Plant Sci. 5, 446-451.
Pubmed: Author and Title
CrossRef: Author and Title
Google Scholar: Author Only Title Only Author and Title

Helliwell, C.A., and Waterhouse, P.M. (2005). Constructs and methods for hairpin RNA-mediated gene silencing in plants. Methods Enzymol. 392, 24-35.
Pubmed: Author and Title
CrossRef: Author and Title
Google Scholar: Author Only Title Only Author and Title

Hofer, R., Dong, L., Andre, F., Ginglinger, J.F., Lugan, R., Gavira, C., Grec, S., Lang, G., Memelink, J., Van der Krol, S., Bouwmeester, H., and Werck-Reichhart, D. (2013). Geraniol hydroxylase and hydroxygeraniol oxidase activities of the CYP76 family of cytochrome P450 enzymes and potential for engineering the early steps of the (seco)iridoid pathway. Metab. Eng. 20, 221-232.
Pubmed: Author and Title
CrossRef: Author and Title
Google Scholar: Author Only Title Only Author and Title

Hutchinson, C.R., Heckendorf, A.H., Straughn, J.L., Daddona, P.E., and Cane, D.E. (1979). Biosynthesis of camptothecin. 3. Definition of strictosamide as the penultimate biosynthetic precursor assisted by carbon-13 and deuterium NMR spectroscopy. Journal of the American Chemical Society 101, 3358-3369.
Pubmed: Author and Title
CrossRef: Author and Title
Google Scholar: Author Only Title Only Author and Title

Irmler, S., Schröder, G., St-Pierre, B., Crouch, N.P., Hotze, M., Schmidt, J., Strack, D., Matern, U., and Schröder, J. (2000). Indole alkaloid biosynthesis in Catharanthus roseus: new enzyme activities and identification of cytochrome P450 CYP72A1 as secologanin synthase. Plant J. 24, 797-804.
Pubmed: Author and Title
CrossRef: Author and Title
Google Scholar: Author Only Title Only Author and Title

Itoh, A., Tanaka, Y., Nagakura, N., Akita, T., Nishi, T., and Tanahashi, T. (2008). Phenolic and iridoid glycosides from Strychnos axillaris. Phytochemistry 69, 1208-1214.
Pubmed: Author and Title
CrossRef: Author and Title
Google Scholar: Author Only Title Only Author and Title

Kumar, K., Kumar, S.R., Dwivedi, V., Rai, A., Shukla, A.K., Shanker, K., and Nagegowda, D.A. (2015). Precursor feeding studies and molecular characterization of geraniol synthase establish the limiting role of geraniol in monoterpene indole alkaloid biosynthesis in Catharanthus roseus leaves. Plant Sci. 239, 56-66.
Pubmed: Author and Title
CrossRef: Author and Title
Google Scholar: Author Only Title Only Author and Title

Leménager, D., Ouelhazi, L., Mahroug, S., Veau, B., St-Pierre, B., Rideau, M., Aguirreolea, J., Burlat, V., and Clastre, M. (2005). Purification, molecular cloning, and cell-specific gene expression of the alkaloid-accumulation associated protein CrPS in Catharanthus roseus. J. Exp. Bot. 56, 1221-1228.
Pubmed: Author and Title
CrossRef: Author and Title
Google Scholar: Author Only Title Only Author and Title

Liu, Y.-Q., Li, W.-Q., Morris-Natschke, S.L., Qian, K., Yang, L., Zhu, G.-X., Wu, X.-B., Chen, A.-L., Zhang, S.-Y., Nan, X., and Lee, K.-H. (2015). Perspectives on Biologically Active Camptothecin Derivatives. Medicinal Res. Rev. 35, 753-789.
Pubmed: Author and Title
CrossRef: Author and Title
Google Scholar: Author Only Title Only Author and Title

Lloyd, G. and McGown, B. (1981) Commercially-feasible micropropagation of Mountain Laurel, Kalmia latifolia, by shoot tip culture. Proc. Int. Plant Prop. Soc. 30, 421-427.
Pubmed: Author and Title
CrossRef: Author and Title
Google Scholar: Author Only Title Only Author and Title

Lopez-Meyer, M., and Nessler, C.L. (1997). Tryptophan decarboxylase is encoded by two autonomously regulated genes in Camptotheca acuminata which are differentially expressed during development and stress. Plant J. 11, 1167-1175.
Pubmed: Author and Title
CrossRef: Author and Title
Google Scholar: Author Only Title Only Author and Title

Lorence, A., and Nessler, C.L. (2004). Camptothecin, over four decades of surprising findings. Phytochemistry 65, 2735-2749.
Pubmed: Author and Title
CrossRef: Author and Title
Google Scholar: Author Only Title Only Author and Title

Marquez, B.L. Gerwick, W.H., and Williamson R.T. (2001) Survey of NMR experiments for the determination of nJ(C,H) heteronuclear coupling constants in small molecules. Magn. Reson. Chem. 39, 499-530.
Pubmed: Author and Title
CrossRef: Author and Title
Google Scholar: Author Only Title Only Author and Title

Miettinen, K., Dong, L., Navrot, N., Schneider, T., Burlat, V., Pollier, J., Woittiez, L., van der Krol, S., Lugan, R., Ilc, T., Verpoorte, R., Oksman-Caldentey, K.M., Martinoia, E., Bouwmeester, H., Goossens, A., Memelink, J., and Werck-Reichhart, D. (2014). The seco-iridoid pathway from Catharanthus roseus. Nature Commun. 5, 3606.
Pubmed: Author and Title
CrossRef: Author and Title
Google Scholar: Author Only Title Only Author and Title

Montoro, P., Maldini, M., Piacente, S., Macchia, M., and Pizza, C. (2010). Metabolite fingerprinting of Camptotheca acuminata and the HPLC-ESI-MS/MS analysis of camptothecin and related alkaloids. J. Pharm. Biomed. Anal. 51, 405-415.
Pubmed: Author and Title
CrossRef: Author and Title
Google Scholar: Author Only Title Only Author and Title

Müller, A.A. and Weigend, M. (1998) Iridoids from Loasa acerifolia. Phytochem. 49,131-135
Pubmed: Author and Title
CrossRef: Author and Title
Google Scholar: Author Only Title Only Author and Title

Munkert, J., Pollier, J., Miettinen, K., Van Moerkercke, A., Payne, R., Muller-Uri, F., Burlat, V., O'Connor, S.E., Memelink, J., Kreis, W., and Goossens, A. (2014). Iridoid Synthase Activity Is Common among the Plant Progesterone 5beta-Reductase Family. Mol. Plant. 8, 136-52.
Pubmed: Author and Title
CrossRef: Author and Title
Google Scholar: Author Only Title Only Author and Title

Murata, J., Roepke, J., Gordon, H., and De Luca, V. (2008). The Leaf Epidermome of Catharanthus roseus Reveals Its Biochemical Specialization. Plant Cell 20, 524-542.
Pubmed: Author and Title
CrossRef: Author and Title
Google Scholar: Author Only Title Only Author and Title

Patthy-Lukáts, Á., Károlyházy, L., Szabó, L.F., and Podányi, B. (1997). First direct and detailed stereochemical analysis of strictosidine. J. Nat. Prod. 60, 69-75.
Pubmed: Author and Title
CrossRef: Author and Title
Google Scholar: Author Only Title Only Author and Title

Rastrelli, L., Caceres, A., Morales, C., De Simone, F., and Aquino, R. (1998) Iridoids from Lippia graveolens. Phytochem. 49, 1829-1832.
Pubmed: Author and Title
CrossRef: Author and Title
Google Scholar: Author Only Title Only Author and Title

Reanmongkol, W., Subhadhirasakul, S., Kongsang, J., Tanchong, M., and Kitti, J. (2000) Analgesic and Antipyretic Activities of n-Butanol Alkaloids Extracted from the Stem Bark Hunteria zeylanica and its Major Constituent, Strictosidinic Acid, in Mice. Pharm. Biol. 38, 68-73.
Pubmed: Author and Title
CrossRef: Author and Title
Google Scholar: Author Only Title Only Author and Title

Saeed, A.I., Bhagabati, N.K., Braisted, J.C., Liang, W., Sharov, V., Howe, E.A., Li, J., Thiagarajan, M., White, J.A., and Quackenbush, J. (2006). [9] TM4 Microarray Software Suite. Methods Enzymol. 411, 134-193.
Pubmed: Author and Title
CrossRef: Author and Title
Google Scholar: Author Only Title Only Author and Title

Salim, V., Yu, F., Altarejos, J., and De Luca, V. (2013). Virus-induced gene silencing identifies Catharanthus roseus 7-deoxyloganic acid-7-hydroxylase, a step in iridoid and monoterpene indole alkaloid biosynthesis. Plant J. 76, 754-765.
Pubmed: Author and Title
CrossRef: Author and Title
Google Scholar: Author Only Title Only Author and Title

Salim, V., Wiens, B., Masada-Atsumi, S., Yu, F., and De Luca, V. (2014). 7-Deoxyloganetic acid synthase catalyzes a key 3 step oxidation to form 7-deoxyloganetic acid in Catharanthus roseus iridoid biosynthesis. Phytochemistry 101, 23-31.
Pubmed: Author and Title
CrossRef: Author and Title
Google Scholar: Author Only Title Only Author and Title

Serrilli, A.M., Ramunno, A., Amicucci, F., Chicarella, V., Santoni, S., Ballero, M., Serafini, M., and Bianco, A. (2008) Iridoidic pattern in

endemic Sardinian plants: the case of Galium species. Nat. Prod. Res. 22, 618-622.
Pubmed: Author and Title
CrossRef: Author and Title
Google Scholar: Author Only Title Only Author and Title

Sheriha, G.M., and Rapoport, H. (1976). Biosynthesis of Camptotheca acuminata alkaloids. Phytochemistry 15, 505-508.
Pubmed: Author and Title
CrossRef: Author and Title
Google Scholar: Author Only Title Only Author and Title

Skaltsounis, A.L., Tillequin, F., Koch, M., Pusset, J. and Chauvière, G. (1989) Iridoids from

Scaevola racemigera. Planta Med. 55, 191-192.

Tamura, K., Peterson, D., Peterson, N., Stecher, G., Nei, M., and Kumar, S. (2011) MEGA5: Molecular Evolutionary Genetics Analysis Using Maximum Likelihood, Evolutionary Distance, and Maximum Parsimony Methods. Mol. Biol. Evol. 28, 2731-2739.
Pubmed: Author and Title
CrossRef: Author and Title
Google Scholar: Author Only Title Only Author and Title

Van Moerkercke, A., Steensma, P., Schweizer, F., Pollier, J., Gariboldi, I., Payne, R., Vanden Bossche, R., Miettinen, K., Espoz, J., Purnama, P.C., Kellner, F., Seppänen-Laakso, T., O'Connor, S.E., Rischer, H., Memelink, J., and Goossens, A. (2015). The bHLH transcription factor BIS1 controls the iridoid branch of the monoterpenoid indole alkaloid pathway in Catharanthus roseus. Proc. Natl. Acad. Sci. U. S. A. 112, 8130-8135.
Pubmed: Author and Title
CrossRef: Author and Title
Google Scholar: Author Only Title Only Author and Title

Wall, M.E., Wani, M.C., Cook, C.E., Palmer, K.H., McPhail, A.T., and Sim, G.A. (1966). Plant Antitumor Agents. I. The Isolation and Structure of Camptothecin, a Novel Alkaloidal Leukemia and Tumor Inhibitor from Camptotheca acuminata. J. Am. Chem. Soc. 88, 3888-3890.
Pubmed: Author and Title
CrossRef: Author and Title
Google Scholar: Author Only Title Only Author and Title

Wink, M. (2003). Evolution of secondary metabolites from an ecological and molecular phylogenetic perspective. Phytochemistry 64, 3-19.
Pubmed: Author and Title
CrossRef: Author and Title
Google Scholar: Author Only Title Only Author and Title

Wright, C.M., van der Merwe, M., DeBrot, A.H., and Bjornsti, M.-A. (2015). DNA Topoisomerase I Domain Interactions Impact Enzyme Activity and Sensitivity to Camptothecin. J. Biol. Chem. 290, 12068-12078.
Pubmed: Author and Title
CrossRef: Author and Title
Google Scholar: Author Only Title Only Author and Title

Yamazaki, M., Mochida, K., Asano, T., Nakabayashi, R., Chiba, M., Udomson, N., Yamazaki, Y., Goodenowe, D.B., Sankawa, U., Yoshida, T., Toyoda, A., Totoki, Y., Sakaki, Y., Góngora-Castillo, E., Buell, C.R., Sakurai, T., and Saito, K. (2013). Coupling Deep Transcriptome Analysis with Untargeted Metabolic Profiling in Ophiorrhiza pumila to Further the Understanding of the Biosynthesis of the Anti-Cancer Alkaloid Camptothecin and Anthraquinones. Plant Cell Physiol. 54, 686-696.
Pubmed: Author and Title
CrossRef: Author and Title
Google Scholar: Author Only Title Only Author and Title

Yamazaki, Y., Sudo, H., Yamazaki, M., Aimi, N., and Saito, K. (2003a). Camptothecin Biosynthetic Genes in Hairy Roots of Ophiorrhiza pumila: Cloning, Characterization and Differential Expression in Tissues and by Stress Compounds. Plant Cell Physiol. 44, 395-403.
Pubmed: Author and Title
CrossRef: Author and Title
Google Scholar: Author Only Title Only Author and Title

Yamazaki, Y., Urano, A., Sudo, H., Kitajima, M., Takayama, H., Yamazaki, M., Aimi, N., and Saito, K. (2003b). Metabolite profiling of alkaloids and strictosidine synthase activity in camptothecin producing plants. Phytochemistry 62, 461-470.
Pubmed: Author and Title
CrossRef: Author and Title
Google Scholar: Author Only Title Only Author and Title

Zhang, T., Li, J., Li, B., Chen, L., Yin, H.L., Liu, S.J., Tian, Y., and Dong, J.X. (2012) Two novel secoiridoid glucosides from Tripterospermum chinense. J. Asian Nat. Prod. Res. 14, 1097-102.
Pubmed: Author and Title
CrossRef: Author and Title
Google Scholar: Author Only Title Only Author and Title

Zhou, Z., Yin, W., Zhang, H., Feng, Z., and Xia, J. (2013) A new iridoid glycoside and potential MRB inhibitory activity of isolated compounds from the rhizomes of Cyperus rotundus L. Nat. Prod Res. 27, 1732-1736.
Pubmed: Author and Title
CrossRef: Author and Title
Google Scholar: Author Only Title Only Author and Title

Ziegler, J., Facchini, P.J. (2008) Alkaloid biosynthesis: metabolism and trafficking. Annu. Rev. Plant Biol. 59, 735-769. Review
Pubmed: Author and Title
CrossRef: Author and Title
Google Scholar: Author Only Title Only Author and Title

Metabolite diversity in alkaloid biosynthesis: A multi-lane (diastereomer) highway for camptothecin synthesis in Camptotheca acuminata

Radin Sadre, Maria Magallanes-Lundback, Sujana Pradhan, Vonny Salim, Alex Mesberg, Arthur Daniel Jones and Dean DellaPenna

Plant Cell; originally published online July 18, 2016;
DOI 10.1105/tpc.16.00193